Rare radiative-and-leptonic B_s-meson decay within and beyond the Standard Model

Ludovico Vittorio (University of Rome Sapienza and INFN, Rome)

EPS-HEP 2025, Marseille – July the 11th, 2025

Mainly based on works with Diego Guadagnoli, Camille Normand and Silvano Simula
[JHEP '23 (2303.02174) and JHEP '23 (2308.00034)]

SAPIENZA UNIVERSITÀ DI ROMA

INFN ROMA
Istituto Nazionale di Fisica Nucleare
Sezione di Roma

MUR
Ministero dell'Università e della Ricerca

Finanziato dall'Unione europea
NextGenerationEU

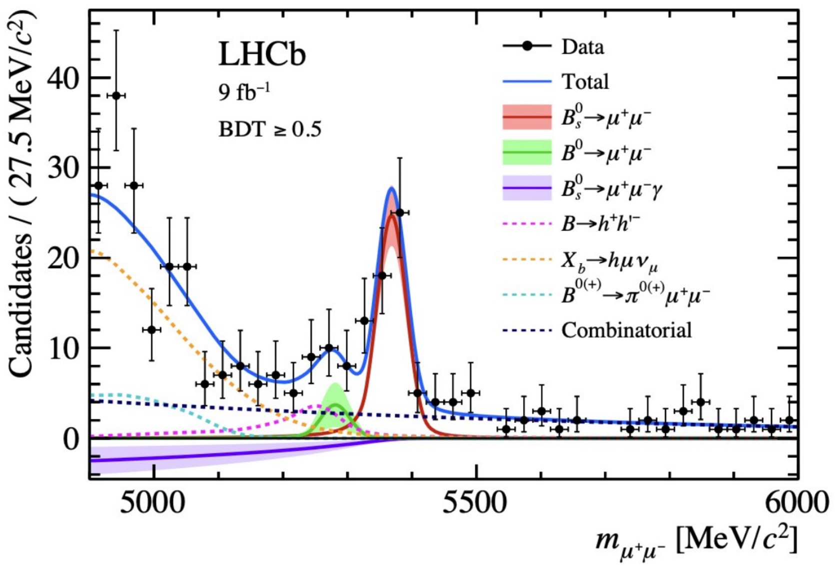

(from LHCb-PAPER-2021-007)

Radiative-and-leptonic Bs decays

A novel possibility to analyze b → s quark transitions is the study of rare radiative-and-leptonic Bs decays. This is experimentally challenging, and the first world limit on this decay was set by LHCb (very close to the SM signal):

$$\mathcal{B}(B_s^0 \to \mu^+\mu^-\gamma) \; < \; 2.0 \times 10^{-9} \quad \left\{ m_{\mu\mu} > 4.9\,\mathrm{GeV}/c^2 \right\}$$

LHCb Collaboration, LHCb-PAPER-2021-007 & LHCb-PAPER-2021-008

Radiative-and-leptonic Bs decays

A novel possibility to analyze b → s quark transitions is the study of rare radiative-and-leptonic Bs decays. This is experimentally challenging, and the first world limit on this decay was set by LHCb (very close to the SM signal):

$$\mathcal{B}(B_s^0 \to \mu^+\mu^-\gamma) \;<\; 2.0\times 10^{-9} \quad \left\{ m_{\mu\mu} > 4.9\,\mathrm{GeV}/c^2 \right\}$$

LHCb Collaboration, LHCb-PAPER-2021-007 & LHCb-PAPER-2021-008

Today (as we will see) new limits in other kinematical regions are available !

Radiative-and-leptonic Bs decays

A novel possibility to analyze b → s quark transitions is the study of rare radiative-and-leptonic Bs decays. This is experimentally challenging, and the first world limit on this decay was set by LHCb (very close to the SM signal):

$$\mathcal{B}(B_s^0 \to \mu^+\mu^-\gamma) \; < \; 2.0 \times 10^{-9} \quad \left\{ m_{\mu\mu} > 4.9\,\mathrm{GeV}/c^2 \right\}$$

LHCb Collaboration, LHCb-PAPER-2021-007 & LHCb-PAPER-2021-008

Today (as we will see) new limits in other kinematical regions are available !

Several advantages from the phenomenological point of view:

1. **No chirality suppression** (thanks to the additional photon): **enhancement w.r.t. the leptonic counterpart**!
2. **Sensitivity to a larger set of WCs**: not only O_{10}(‘), also O_7(‘) and O_9(‘) (*reminder: O_9(‘) and O_{10}(‘) are particularly relevant @ high-q2*)
3. **Two ways to detect it experimentally:**

- ***directly*** **(*i.e.* w/ photon reconstruction) [LHCb Coll., JHEP ‘24 (2404.03375)]**
- ***indirectly*** **(*i.e.* w/out photon reconstruction) [Dettori et al, PLB ’17 (1610.00629)]**

Radiative-and-leptonic decays in Effective Field Theory

Standard WET approach:

$$\mathcal{H} = -\frac{4G_F}{\sqrt{2}}\lambda_{\rm CKM}\left[\frac{\alpha_{em}}{4\pi}\left(\sum_i C_i\mathcal{O}_i + \sum_i C_i'\mathcal{O}_i'\right)\right]$$

$$\mathcal{O}_7 = em_{q_j}(\bar{q}_{Li}\sigma_{\mu\nu}q_{Rj})F^{\mu\nu}$$

$$\mathcal{O}_9^k = (\bar{q}_{Li}\gamma^\mu q_{Lj})(\bar{\ell}_k\gamma^\mu\ell_k),$$

$$\mathcal{O}_{10}^k = (\bar{q}_{Li}\gamma^\mu q_{Lj})(\bar{\ell}_k\gamma^\mu\gamma_5\ell_k),$$

Radiative-and-leptonic decays in Effective Field Theory

Standard WET approach:

$$\mathcal{H} = -\frac{4G_F}{\sqrt{2}}\lambda_{\text{CKM}}\left[\frac{\alpha_{em}}{4\pi}\left(\sum_i C_i\mathcal{O}_i + \sum_i C_i^{'}\mathcal{O}_i^{'}\right)\right]$$

$$\mathcal{O}_7 = e m_{q_j}(\bar{q}_{Li}\sigma_{\mu\nu}q_{Rj})F^{\mu\nu}$$

$$\mathcal{O}_9^k = (\bar{q}_{Li}\gamma^\mu q_{Lj})(\bar{\ell}_k\gamma^\mu\ell_k),$$

$$\mathcal{O}_{10}^k = (\bar{q}_{Li}\gamma^\mu q_{Lj})(\bar{\ell}_k\gamma^\mu\gamma_5\ell_k),$$

At the end of the day, we will be interested in analyzing:

$$H_{\text{eff}}^{b\to sl^+l^-} = \frac{G_F}{\sqrt{2}}\frac{\alpha_{\text{em}}}{2\pi}V_{tb}V_{ts}^*\left[-2im_b\frac{C_{7\gamma}(\mu)}{q^2}\cdot\bar{s}\sigma_{\mu\nu}q^\nu(1+\gamma_5)b\cdot\bar{l}\gamma^\mu l + C_{9V}(\mu)\cdot\bar{s}\gamma_\mu(1-\gamma_5)b\cdot\bar{l}\gamma^\mu l + C_{10A}(\mu)\cdot\bar{s}\gamma_\mu(1-\gamma_5)b\cdot\bar{l}\gamma^\mu\gamma_5 l\right]$$

Melikhov and Nikitin, Phys. Rev. D 70 (2004) 114028
Kozachuk, Melikhov and Nikitin, Phys. Rev. D 97 (2018) 053007

Radiative-and-leptonic decays in Effective Field Theory

Standard WET approach:

$$\mathcal{H} = -\frac{4G_F}{\sqrt{2}}\lambda_{\text{CKM}}\left[\frac{\alpha_{em}}{4\pi}\left(\sum_i C_i \mathcal{O}_i + \sum_i C_i^{'}\mathcal{O}_i^{'}\right)\right]$$

$$\mathcal{O}_7 = e m_{q_j}(\bar{q}_{Li}\sigma_{\mu\nu}q_{Rj})F^{\mu\nu}$$

$$\mathcal{O}_9^k = (\bar{q}_{Li}\gamma^\mu q_{Lj})(\bar{\ell}_k\gamma^\mu\ell_k),$$

$$\mathcal{O}_{10}^k = (\bar{q}_{Li}\gamma^\mu q_{Lj})(\bar{\ell}_k\gamma^\mu\gamma_5\ell_k),$$

At the end of the day, we will be interested in analyzing:

$$H_{\text{eff}}^{b\to sl^+l^-} = \frac{G_F}{\sqrt{2}}\frac{\alpha_{\text{em}}}{2\pi}V_{tb}V_{ts}^*\left[-2im_b\frac{C_{7\gamma}(\mu)}{q^2}\cdot\bar{s}\sigma_{\mu\nu}q^\nu(1+\gamma_5)b\cdot\bar{l}\gamma^\mu l \right.$$
$$\left. + C_{9V}(\mu)\cdot\bar{s}\gamma_\mu(1-\gamma_5)b\cdot\bar{l}\gamma^\mu l + C_{10A}(\mu)\cdot\bar{s}\gamma_\mu(1-\gamma_5)b\cdot\bar{l}\gamma^\mu\gamma_5 l\right]$$

$$H_{\text{eff}}^{b\to s\bar{c}c} = -\frac{G_F}{\sqrt{2}}V_{cb}V_{cs}^*\left\{C_1(\mu)\mathcal{O}_1 + C_2(\mu)\mathcal{O}_2\right\}$$

$$\mathcal{O}_1 = \bar{s}^j\gamma_\mu(1-\gamma_5)c^i\,\bar{c}^i\gamma^\mu(1-\gamma_5)b^j, \qquad \mathcal{O}_2 = \bar{s}^i\gamma_\mu(1-\gamma_5)c^i\,\bar{c}^j\gamma^\mu(1-\gamma_5)b^j,$$

Melikhov and Nikitin, Phys. Rev. D 70 (2004) 114028
Kozachuk, Melikhov and Nikitin, Phys. Rev. D 97 (2018) 053007

Radiative-and-leptonic decays in Effective Field Theory

5 different classes of diagrams:

1. Direct Emission (DE) of the photon from valence quarks
2. DE of the virtual photon from valence quarks
3. Bremsstrahlung
4. Charm loops diagrams
5. Weak annihilation diagram

$$H_{\rm eff}^{b\to sl^+l^-} = \frac{G_F}{\sqrt{2}}\frac{\alpha_{\rm em}}{2\pi}V_{tb}V_{ts}^*\left[-2im_b\frac{C_{7\gamma}(\mu)}{q^2}\cdot\bar{s}\sigma_{\mu\nu}q^\nu(1+\gamma_5)b\cdot\bar{l}\gamma^\mu l \right.$$
$$\left.+C_{9V}(\mu)\cdot\bar{s}\gamma_\mu(1-\gamma_5)b\cdot\bar{l}\gamma^\mu l + C_{10A}(\mu)\cdot\bar{s}\gamma_\mu(1-\gamma_5)b\cdot\bar{l}\gamma^\mu\gamma_5 l\right]$$

$$H_{\rm eff}^{b\to s\bar{c}c} = -\frac{G_F}{\sqrt{2}}V_{cb}V_{cs}^*\left\{C_1(\mu)\mathcal{O}_1 + C_2(\mu)\mathcal{O}_2\right\}$$

$$\mathcal{O}_1 = \bar{s}^j\gamma_\mu(1-\gamma_5)c^i\,\bar{c}^i\gamma^\mu(1-\gamma_5)b^j, \qquad \mathcal{O}_2 = \bar{s}^i\gamma_\mu(1-\gamma_5)c^i\,\bar{c}^j\gamma^\mu(1-\gamma_5)b^j,$$

Melikhov and Nikitin, Phys. Rev. D 70 (2004) 114028
Kozachuk, Melikhov and Nikitin, Phys. Rev. D 97 (2018) 053007

Radiative-and-leptonic decays in Effective Field Theory

5 different classes of diagrams:

1. Direct Emission (DE) of the photon from valence quarks
2. DE of the virtual photon from valence quarks
3. Bremsstrahlung
4. Charm loops diagrams
5. Weak annihilation diagram

● = $\mathcal{O}_{9,10}$

Example:

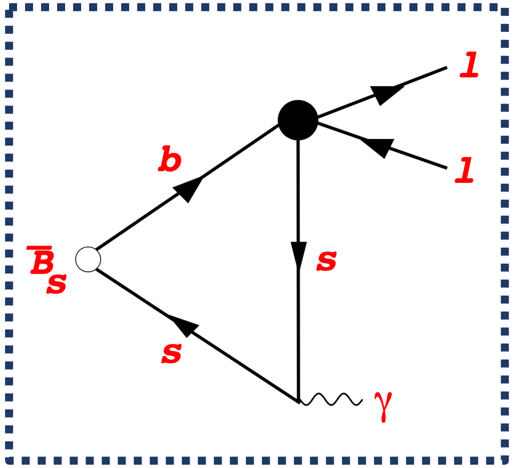

$$H_{\text{eff}}^{b\to s l^+ l^-} = \frac{G_F}{\sqrt{2}} \frac{\alpha_{\text{em}}}{2\pi} V_{tb} V_{ts}^* \Big[-2 i m_b \frac{C_{7\gamma}(\mu)}{q^2} \cdot \bar{s}\sigma_{\mu\nu} q^\nu (1+\gamma_5)\, b \cdot \bar{l}\gamma^\mu l + C_{9V}(\mu) \cdot \bar{s}\gamma_\mu (1-\gamma_5)\, b \cdot \bar{l}\gamma^\mu l + C_{10A}(\mu) \cdot \bar{s}\gamma_\mu (1-\gamma_5)\, b \cdot \bar{l}\gamma^\mu \gamma_5 l \Big]$$

$$H_{\text{eff}}^{b\to s\bar{c}c} = -\frac{G_F}{\sqrt{2}} V_{cb} V_{cs}^* \left\{ C_1(\mu)\mathcal{O}_1 + C_2(\mu)\mathcal{O}_2 \right\}$$

$$\mathcal{O}_1 = \bar{s}^j \gamma_\mu (1-\gamma_5) c^i\, \bar{c}^i \gamma^\mu (1-\gamma_5) b^j, \qquad \mathcal{O}_2 = \bar{s}^i \gamma_\mu (1-\gamma_5) c^i\, \bar{c}^j \gamma^\mu (1-\gamma_5) b^j,$$

Melikhov and Nikitin, Phys. Rev. D 70 (2004) 114028
Kozachuk, Melikhov and Nikitin, Phys. Rev. D 97 (2018) 053007

Radiative-and-leptonic decays in Effective Field Theory

5 different classes of diagrams:

1. Direct Emission (DE) of the photon from valence quarks
2. DE of the virtual photon from valence quarks
3. Bremsstrahlung
4. Charm loops diagrams
5. Weak annihilation diagram

Example:

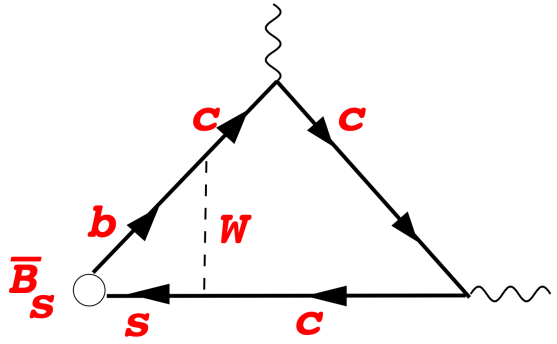

$$H_{\rm eff}^{b\to s l^+ l^-} = \frac{G_F}{\sqrt{2}} \frac{\alpha_{\rm em}}{2\pi} V_{tb} V_{ts}^* \left[-2 i m_b \frac{C_{7\gamma}(\mu)}{q^2} \cdot \bar{s}\sigma_{\mu\nu} q^\nu (1+\gamma_5) b \cdot \bar{l}\gamma^\mu l + C_{9V}(\mu) \cdot \bar{s}\gamma_\mu (1-\gamma_5) b \cdot \bar{l}\gamma^\mu l + C_{10A}(\mu) \cdot \bar{s}\gamma_\mu (1-\gamma_5) b \cdot \bar{l}\gamma^\mu \gamma_5 l \right]$$

$$H_{\rm eff}^{b\to s\bar{c}c} = -\frac{G_F}{\sqrt{2}} V_{cb} V_{cs}^* \left\{ C_1(\mu)\mathcal{O}_1 + C_2(\mu)\mathcal{O}_2 \right\}$$

$$\mathcal{O}_1 = \bar{s}^j \gamma_\mu (1-\gamma_5) c^i \, \bar{c}^i \gamma^\mu (1-\gamma_5) b^j, \qquad \mathcal{O}_2 = \bar{s}^i \gamma_\mu (1-\gamma_5) c^i \, \bar{c}^j \gamma^\mu (1-\gamma_5) b^j,$$

Melikhov and Nikitin, Phys. Rev. D 70 (2004) 114028
Kozachuk, Melikhov and Nikitin, Phys. Rev. D 97 (2018) 053007

Radiative-and-leptonic decays in Effective Field Theory

5 different classes of diagrams:

1. Direct Emission (DE) of the photon from valence quarks
2. DE of the virtual photon from valence quarks
3. Bremsstrahlung
4. Charm loops diagrams
5. Weak annihilation diagram

Example:

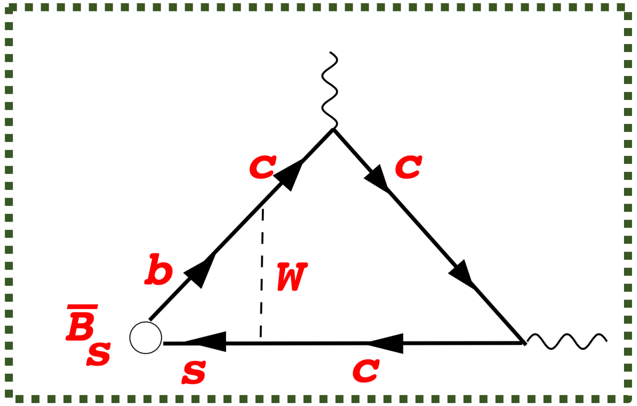

Important issue: **<u>only 4 diagrams</u> give the most important contribution at high-q2, *i.e.***

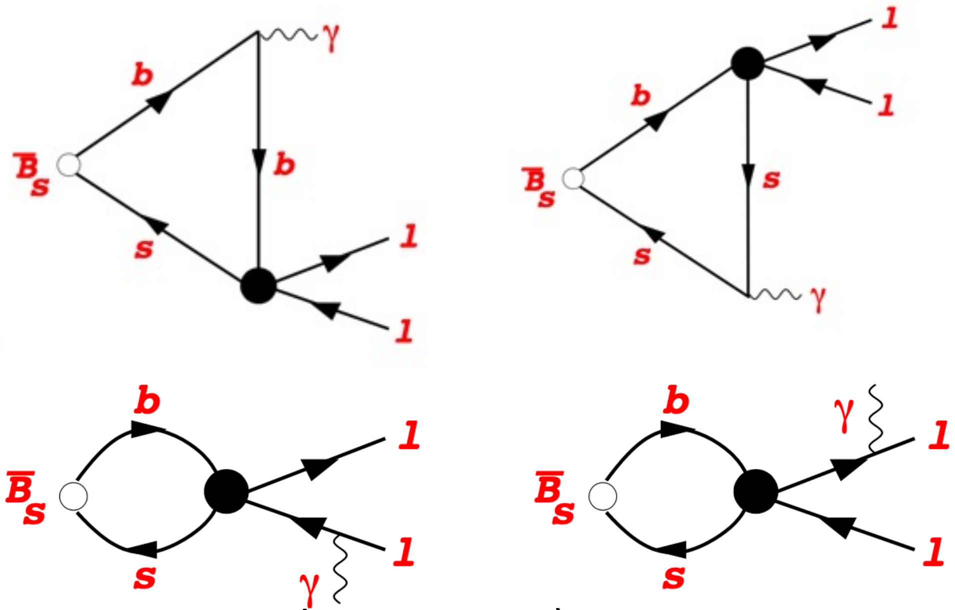

$\bullet = O_{9,10}$

Available results for the $B_s \to \gamma$ hadronic FFs

$$\langle\gamma(k,\epsilon)|O_\mu^V|\bar{B}_q(p_B)\rangle = s_e(P_\mu^\perp V_\perp(q^2) - P_\mu^\parallel (V_\parallel(q^2) + Q_{\bar{B}_q} f_{B_q}^{(pt)}) - P_\mu^{\rm Low} Q_{\bar{B}_q} f_{B_q}^{(pt)})$$

$$P_{\mu\rho}^\perp \equiv \varepsilon_{\mu\rho\beta\gamma}(p_B)^\beta k^\gamma \ , \quad P_{\mu\rho}^\parallel \equiv i\,(p_B \cdot k\, g_{\mu\rho} - k_\mu\,(p_B)_\rho) \ , \quad P_{\mu\rho}^{\rm Low} \equiv i(p_B)_\mu (p_B)_\rho$$

Janowski, Pullin and Zwicky, JHEP '21 (2106.13616)

Available results for the $B_s \to \gamma$ hadronic FFs

$$\langle \gamma(k,\epsilon)|O_\mu^V|\bar{B}_q(p_B)\rangle = s_e(P_\mu^\perp V_\perp(q^2) - P_\mu^\parallel (V_\parallel(q^2) + Q_{\bar{B}_q} f_{B_q}^{(pt)}) - P_\mu^{\rm Low} Q_{\bar{B}_q} f_{B_q}^{(pt)})$$

$$P_{\mu\rho}^\perp \equiv \varepsilon_{\mu\rho\beta\gamma}(p_B)^\beta k^\gamma \ , \quad P_{\mu\rho}^\parallel \equiv i\,(p_B \cdot k\, g_{\mu\rho} - k_\mu\,(p_B)_\rho) \ , \quad P_{\mu\rho}^{\rm Low} \equiv i(p_B)_\mu (p_B)_\rho$$

$$f_{B_q}^{(pt)} = \frac{m_{B_q} f_{B_q}}{k \cdot p_B} = \frac{2 f_{B_q}/m_{B_q}}{1 - q^2/m_{B_q}^2}$$

Janowski, Pullin and Zwicky, JHEP '21 (2106.13616)

Available results for the $B_s \to \gamma$ hadronic FFs

$$\langle \gamma(k,\epsilon)|O^V_\mu|\bar{B}_q(p_B)\rangle = s_e(P^\perp_\mu V_\perp(q^2) - P^\parallel_\mu (V_\parallel(q^2) + Q_{\bar{B}_q} f^{(pt)}_{B_q}) - P^{\text{Low}}_\mu Q_{\bar{B}_q} f^{(pt)}_{B_q})$$

$$P^\perp_{\mu\rho} \equiv \varepsilon_{\mu\rho\beta\gamma}(p_B)^\beta k^\gamma\ , \quad P^\parallel_{\mu\rho} \equiv i\,(p_B\cdot k\, g_{\mu\rho} - k_\mu\,(p_B)_\rho)\ , \quad P^{\text{Low}}_{\mu\rho} \equiv i(p_B)_\mu (p_B)_\rho$$

$$f^{(pt)}_{B_q} = \frac{m_{B_q} f_{B_q}}{k\cdot p_B} = \frac{2 f_{B_q}/m_{B_q}}{1 - q^2/m^2_{B_q}}$$

Janowski, Pullin and Zwicky, JHEP '21 (2106.13616)

- **First determination on the lattice**

  Frezzotti et al, ETMC Collaboration, PRD '24 [2402.03262] (high-q2 computation)

  (methodological inputs also from Giusti et al., PRD '23 [2302.01298] and 2505.11757)

Available results for the $B_s \to \gamma$ hadronic FFs

$$\langle \gamma(k,\epsilon)|O_\mu^V|\bar{B}_q(p_B)\rangle = s_e\left(P_\mu^\perp V_\perp(q^2) - P_\mu^\parallel\left(V_\parallel(q^2) + Q_{\bar{B}_q} f_{B_q}^{(pt)}\right) - P_\mu^{\rm Low} Q_{\bar{B}_q} f_{B_q}^{(pt)}\right)$$

$$P_{\mu\rho}^\perp \equiv \varepsilon_{\mu\rho\beta\gamma}(p_B)^\beta k^\gamma\ , \quad P_{\mu\rho}^\parallel \equiv i\left(p_B\cdot k\, g_{\mu\rho} - k_\mu (p_B)_\rho\right)\ , \quad P_{\mu\rho}^{\rm Low} \equiv i(p_B)_\mu (p_B)_\rho$$

$$f_{B_q}^{(pt)} = \frac{m_{B_q} f_{B_q}}{k\cdot p_B} = \frac{2 f_{B_q}/m_{B_q}}{1-q^2/m_{B_q}^2}$$

Janowski, Pullin and Zwicky, JHEP '21 (2106.13616)

- **First determination on the lattice**
  Frezzotti et al, ETMC Collaboration, PRD '24 [2402.03262] (high-q2 computation)
  (methodological inputs also from Giusti et al., PRD '23 [2302.01298] and 2505.11757)

- **Other determinations using different theoretical frameworks:**
  - Kozachuk, Melikhov and Nikitin (KMN) [PRD '18 (1712.07926)]
  - Dubnicka, Dubnickova, Ivanov, Liptaj, Santorelli, Tran (DDILST) [PRD '19 (1808.06261)]
  - Beneke, Bobeth and Wang (BBW) [JHEP '20 (2008.12494)] (low-q2 computation)
  - Janowski, Pullin and Zwicky (JPZ) [JHEP'21 (2106.13616)]
  - Guadagnoli, Normand, Simula, LV (GNSV) [JHEP '23 (2303.02174)] (high-q2 computation)

Available results for the $B_s \to \gamma$ hadronic FFs

$$\langle \gamma(k,\epsilon)|O_\mu^V|\bar{B}_q(p_B)\rangle = s_e(P_\mu^\perp V_\perp(q^2) - P_\mu^\parallel (V_\parallel(q^2) + Q_{\bar{B}_q} f_{B_q}^{(pt)}) - P_\mu^{\rm Low} Q_{\bar{B}_q} f_{B_q}^{(pt)})$$

$$P_{\mu\rho}^\perp \equiv \varepsilon_{\mu\rho\beta\gamma}(p_B)^\beta k^\gamma \,, \quad P_{\mu\rho}^\parallel \equiv i\,(p_B\cdot k\, g_{\mu\rho} - k_\mu\,(p_B)_\rho)\,, \quad P_{\mu\rho}^{\rm Low} \equiv i(p_B)_\mu (p_B)_\rho$$

$$f_{B_q}^{(pt)} = \frac{m_{B_q} f_{B_q}}{k\cdot p_B} = \frac{2 f_{B_q}/m_{B_q}}{1 - q^2/m_{B_q}^2}$$

Janowski, Pullin and Zwicky, JHEP '21 (2106.13616)

- **First determination on the lattice**

  Frezzotti et al, ETMC Collaboration, PRD '24 [2402.03262] (high-q2 computation)
  (methodological inputs also from Giusti et al., PRD '23 [2302.01298] and 2505.11757)

- **Other determinations using different theoretical frameworks:**

  - Kozachuk, Melikhov and Nikitin (KMN) [PRD '18 (1712.07926)]
  - Dubnicka, Dubnickova, Ivanov, Liptaj, Santorelli, Tran (DDILST) [PRD '19 (1808.06261)]
  - Beneke, Bobeth and Wang (BBW) [JHEP '20 (2008.12494)] (low-q2 computation)
  - Janowski, Pullin and Zwicky (JPZ) [JHEP'21 (2106.13616)]
  - Guadagnoli, Normand, Simula, LV (GNSV) [JHEP '23 (2303.02174)] (high-q2 computation)

→ **Main idea**: *HQET scaling of FFs parameters from the Ds-sector to the Bs-sector, starting from Lattice QCD (LQCD) data available for the Ds-sector @ high-q2*

Methodological overview of the GNSV approach to hadronic FFs

Each FF obeys a dispersion relation of this form:

$$V_{\perp[\|]}^{D_s}(q^2) = \frac{1}{\pi}\int_0^\infty dt \frac{\mathrm{Im}[V_{\perp[\|]}^{D_s}(t)]}{t-q^2} = \frac{r_{\perp[\|]}^{D_s^*[D_{s1}]}}{1-q^2/m_{D_s^*[D_{s1}]}^2} + \dots$$

$$\left[\begin{aligned} r_\perp^{D_s^*} &= \frac{m_{D_s} f_{D_s^*}}{m_{D_s^*}} g_{D_s^* D_s \gamma}, \\ r_\|^{D_{s1}} &= \frac{m_{D_s} f_{D_{s1}}}{m_{D_{s1}}} g_{D_{s1} D_s \gamma} \end{aligned}\right]$$

Methodological overview of the GNSV approach to hadronic FFs

Each FF obeys a dispersion relation of this form:

$$V^{D_s}_{\perp[\|]}(q^2) = \frac{1}{\pi}\int_0^\infty dt \frac{\mathrm{Im}[V^{D_s}_{\perp[\|]}(t)]}{t-q^2} = \frac{r^{D_s^*[D_{s1}]}_{\perp[\|]}}{1-q^2/m^2_{D_s^*[D_{s1}]}} + \dots$$

$$\left[\begin{aligned} r^{D_s^*}_{\perp} &= \frac{m_{D_s} f_{D_s^*}}{m_{D_s^*}} g_{D_s^* D_s \gamma}, \\ r^{D_{s1}}_{\|} &= \frac{m_{D_s} f_{D_{s1}}}{m_{D_{s1}}} g_{D_{s1} D_s \gamma} \end{aligned}\right]$$

Opportunity to test different pole structures ($\chi = \perp, \|$): for instance

P fit

$$V_\chi(q^2) = \frac{r_{\chi 1}}{1-q^2/m^2_{\mathrm{ph1}}},$$

PP fit

$$V_\chi(q^2) = \frac{r_{\chi 1}}{1-q^2/m^2_{\mathrm{ph1}}} + \frac{r_{\chi 2}}{1-q^2/m^2_{\chi 2}}$$

Methodological overview of the GNSV approach to hadronic FFs

Each FF obeys a dispersion relation of this form:

$$V_{\perp[\|]}^{D_s}(q^2) = \frac{1}{\pi}\int_0^\infty dt \frac{\mathrm{Im}[V_{\perp[\|]}^{D_s}(t)]}{t-q^2} = \frac{r_{\perp[\|]}^{D_s^*[D_{s1}]}}{1-q^2/m^2_{D_s^*[D_{s1}]}} + \dots$$

$$\left[\begin{array}{l} r_\perp^{D_s^*} = \frac{m_{D_s} f_{D_s^*}}{m_{D_s^*}} g_{D_s^* D_s \gamma}, \\ r_\|^{D_{s1}} = \frac{m_{D_s} f_{D_{s1}}}{m_{D_{s1}}} g_{D_{s1} D_s \gamma} \end{array}\right]$$

Opportunity to test different pole structures ($\chi = \perp, \|$): for instance

P fit

$$V_\chi(q^2) = \frac{r_{\chi 1}}{1-q^2/m^2_{\mathrm{ph1}}},$$

PP fit

$$V_\chi(q^2) = \frac{r_{\chi 1}}{1-q^2/m^2_{\mathrm{ph1}}} + \frac{r_{\chi 2}}{1-q^2/m^2_{\chi 2}}$$

General methodology**: the free parameters of each ansaetze can be determined through fits to lattice data *at high-q2* !**

Methodological overview of the GNSV approach to hadronic FFs

Each FF obeys a dispersion relation of this form:

$$V_{\perp[\|]}^{D_s}(q^2) = \frac{1}{\pi}\int_0^\infty dt \frac{\mathrm{Im}[V_{\perp[\|]}^{D_s}(t)]}{t-q^2} = \frac{r_{\perp[\|]}^{D_s^*[D_{s1}]}}{1-q^2/m^2_{D_s^*[D_{s1}]}} + \ldots$$

$$\left[\; r_\perp^{D_s^*} = \frac{m_{D_s} f_{D_s^*}}{m_{D_s^*}} g_{D_s^* D_s \gamma}, \qquad r_\|^{D_{s1}} = \frac{m_{D_s} f_{D_{s1}}}{m_{D_{s1}}} g_{D_{s1} D_s \gamma} \;\right]$$

Opportunity to test different pole structures ($\chi = \perp, \|$): for instance

P fit

$$V_\chi(q^2) = \frac{r_{\chi 1}}{1-q^2/m^2_{\mathrm{ph1}}},$$

PP fit

$$V_\chi(q^2) = \frac{r_{\chi 1}}{1-q^2/m^2_{\mathrm{ph1}}} + \frac{r_{\chi 2}}{1-q^2/m^2_{\chi 2}}$$

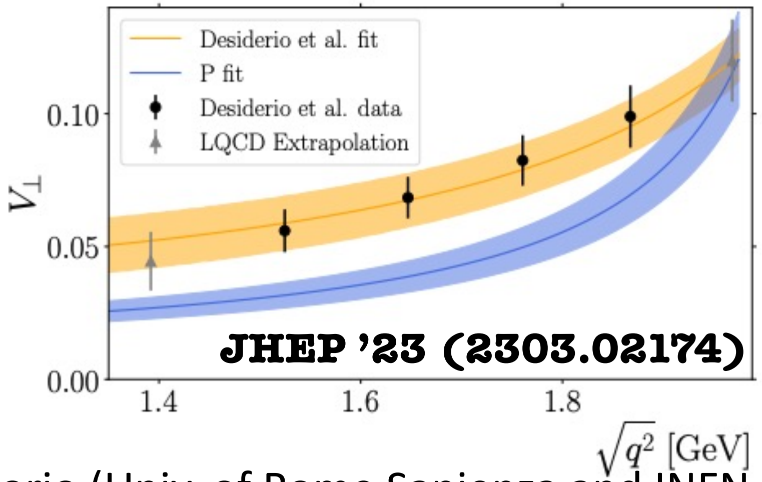

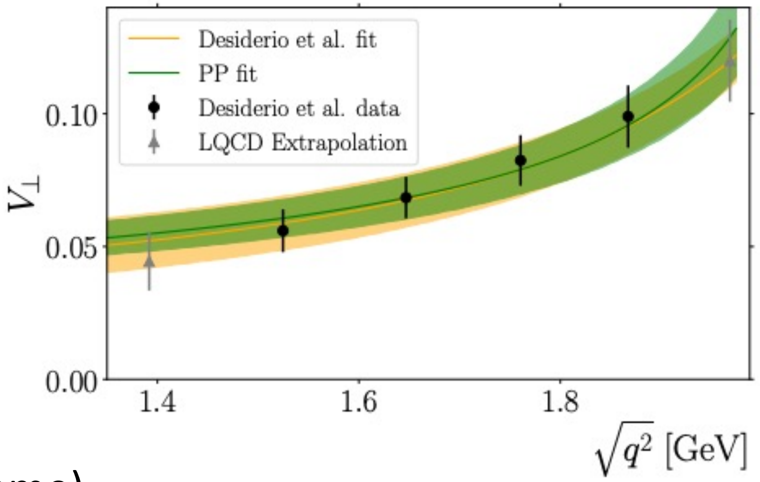

LQCD data from Desiderio et al., PRD '21 (2006.05358)

P fit: $r_\perp^{D_s^*} = 0.015(2)$, $\chi^2 = 32$

PP fit: $r_{\perp 1} = 0.009 \pm 0.003$, $r_{\perp 2} = 0.029 \pm 0.005$, $\chi^2 = 1.5$

Methodological overview of the GNSV approach to hadronic FFs

Once inferred the residues in the Ds sector, the extrapolation to the Bs-sector is based on the 3-couplings:

$$\begin{aligned} g_{D_s^* D_s \gamma} &= Q_s \mu_s^{\perp 1} + Q_c \mu_c^{\perp 1} \,, \quad g_{D_{s1} D_s \gamma} &= -Q_s \mu_s^{\parallel} + Q_c \mu_c^{\parallel} \,, \\ g_{B_s^* B_s \gamma} &= Q_s \mu_s^{\perp 1} + Q_b \mu_b^{\perp 1} \,, \quad g_{B_{s1} B_s \gamma} &= -Q_s \mu_s^{\parallel} + Q_b \mu_b^{\parallel} \,, \end{aligned}$$

$$\left[\mu_c^{\parallel} = \frac{m_s}{m_c} \mu_s^{\parallel} \,, \qquad \mu_b^{\parallel} = \frac{m_s}{m_b} \mu_s^{\parallel} \,. \right]$$

Methodological overview of the GNSV approach to hadronic FFs

Once inferred the residues in the Ds sector, the extrapolation to the Bs-sector is based on the 3-couplings:

$$
\begin{aligned}
g_{D_s^* D_s \gamma} &= Q_s \mu_s^{\perp 1} + Q_c \mu_c^{\perp 1}\,, \quad g_{D_{s1} D_s \gamma} = -Q_s \mu_s^{\parallel} + Q_c \mu_c^{\parallel}\,, \\
g_{B_s^* B_s \gamma} &= Q_s \mu_s^{\perp 1} + Q_b \mu_b^{\perp 1}\,, \quad g_{B_{s1} B_s \gamma} = -Q_s \mu_s^{\parallel} + Q_b \mu_b^{\parallel}\,,
\end{aligned}
$$

$$
\left[\; \mu_c^{\parallel} = \frac{m_s}{m_c}\mu_s^{\parallel}\,, \qquad \mu_b^{\parallel} = \frac{m_s}{m_b}\mu_s^{\parallel}\,. \;\right]
$$

Quark magnetic moments		$B_s \to \gamma$ FFs parameters	
$\mu_s^{\perp 1}$	$-0.22(8)$	$r_{\perp 1}^{B_s}$	0.017 ± 0.006
$\mu_b^{\perp 1}$	$-0.019(6)$	$r_{\perp 2}^{B_s}$	0.088 ± 0.030
$\mu_s^{\perp 2}$	$-2.6(8)$	$r_{\parallel}^{B_s}$	-0.043 ± 0.004
$\mu_b^{\perp 2}$	$-0.22(6)$	$\rho(r_{\perp 1}, r_{\perp 2})$	-0.21
$\mu_s^{\parallel}$	$-0.46(4)$		
$\mu_b^{\parallel}$	$-0.038(3)$	**JHEP '23**	**(2303.02174)**

Starting from LQCD data in Desiderio et al., PRD '21 (2006.05358)

Methodological overview of the GNSV approach to hadronic FFs

Once inferred the residues in the Ds sector, the extrapolation to the Bs-sector is based on the 3-couplings:

$$g_{D_s^* D_s \gamma} = Q_s \mu_s^{\perp 1} + Q_c \mu_c^{\perp 1} \, , \quad g_{D_{s1} D_s \gamma} = -Q_s \mu_s^{\parallel} + Q_c \mu_c^{\parallel} \, ,$$

$$g_{B_s^* B_s \gamma} = Q_s \mu_s^{\perp 1} + Q_b \mu_b^{\perp 1} \, , \quad g_{B_{s1} B_s \gamma} = -Q_s \mu_s^{\parallel} + Q_b \mu_b^{\parallel} \, ,$$

$$\left[\mu_c^{\parallel} = \frac{m_s}{m_c} \mu_s^{\parallel} \, , \qquad \mu_b^{\parallel} = \frac{m_s}{m_b} \mu_s^{\parallel} \, . \right]$$

Final ingredient for the computation of BR(Bs → *μμɣ*) @ high-q2: *charmonia* !

All broad-charmonium states are included as properly normalized Breit-Wigner (BW) poles, that shift the Wilson coefficient C_9 in this way:

$$C_9 \to C_9 - \frac{9\pi}{\alpha^2} \bar{C} \sum_V |\eta_V| e^{i\delta_V} \frac{\hat{m}_V \, \mathcal{B}(V \to \mu^+ \mu^-) \, \hat{\Gamma}^V_{\text{tot}}}{\hat{q}^2 - \hat{m}_V^2 + i \hat{m}_V \hat{\Gamma}^V_{\text{tot}}}$$

Kruger and Sehgal, PLB '96 (hep-ph/9603237)

$$\bar{C} = C_1 + C_2/3 + C_3 + C_4/3 + C_5 + C_6/3$$

Values taken from
Beneke, Bobeth and Wang, JHEP '20 [2008.12494]

$m_{\psi(2S)}$	3.686 GeV	PDG '22	$\Gamma_{\psi(2S)}$	0.294×10^{-3} GeV	PDG '22
$m_{\psi(3770)}$	3.774 GeV		$\Gamma_{\psi(3770)}$	27.2×10^{-3} GeV	
$m_{\psi(4040)}$	4.039 GeV		$\Gamma_{\psi(4040)}$	80×10^{-3} GeV	
$m_{\psi(4160)}$	4.191 GeV		$\Gamma_{\psi(4160)}$	70×10^{-3} GeV	
$m_{\psi(4415)}$	4.421 GeV		$\Gamma_{\psi(4415)}$	62×10^{-3} GeV	
$\mathcal{B}(\psi(2S) \to \ell\ell)$	8.0×10^{-3}	PDG '22	$\delta_{\psi(2S)}$	0	BES Coll.
$\mathcal{B}(\psi(3770) \to \ell\ell)$	9.6×10^{-6}		$\delta_{\psi(3770)}$	0	
$\mathcal{B}(\psi(4040) \to \ell\ell)$	10.7×10^{-6}		$\delta_{\psi(4040)}$	$133 \times \pi/180$	
$\mathcal{B}(\psi(4160) \to \ell\ell)$	6.9×10^{-6}		$\delta_{\psi(4160)}$	$301 \times \pi/180$	
$\mathcal{B}(\psi(4415) \to \ell\ell)$	2.0×10^{-5}		$\delta_{\psi(4415)}$	$246 \times \pi/180$	

arXiv:0705.4500

The full formula for BR(Bs → $\mu\mu\gamma$)

$$\frac{d^2\Gamma^{(1)}}{d\hat{s}\,d\hat{t}} = \frac{G_F^2\,\alpha_{em}^3\,M_1^5}{2^{10}\,\pi^4}\,\left|V_{tb}\,V_{tq}^*\right|^2\left[x^2\,B_0\left(\hat{s},\,\hat{t}\right)\,+\,x\,\xi\left(\hat{s},\hat{t}\right)\,\tilde{B}_1\left(\hat{s},\,\hat{t}\right)\,+\,\xi^2\left(\hat{s},\hat{t}\right)\,\tilde{B}_2\left(\hat{s},\,\hat{t}\right)\right], \qquad (6.1)$$

$$B_0\left(\hat{s},\,\hat{t}\right) = \left(\hat{s}\,+\,4\hat{m}_l^2\right)\left(F_1\left(\hat{s}\right)\,+\,F_2\left(\hat{s}\right)\right)\,-\,8\hat{m}_l^2\,\left|C_{10A}(\mu)\right|^2\left(F_V^2\left(q^2\right)\,+\,F_A^2\left(q^2\right)\right),$$

$$\tilde{B}_1\left(\hat{s},\,\hat{t}\right) = 8\,\Big[\hat{s}\,F_V(q^2)\,F_A(q^2)\,Re\left(C_{9V}^{eff\,*}(\mu,q^2)\,C_{10A}(\mu)\right)$$
$$+\,\hat{m}_b\,F_V(q^2)\,Re\left(C_{7\gamma}^*(\mu)\,\bar{F}_{TA}^*(q^2)\,C_{10A}(\mu)\right)+\hat{m}_b\,F_A(q^2)\,Re\left(C_{7\gamma}^*(\mu)\,\bar{F}_{TV}^*(q^2)\,C_{10A}(\mu)\right)\Big],$$

$$\tilde{B}_2\left(\hat{s},\,\hat{t}\right) = \hat{s}\,\left(F_1\left(\hat{s}\right)\,+\,F_2\left(\hat{s}\right)\right),$$

$$F_1\left(\hat{s}\right) = \left(\left|C_{9V}^{\rm eff}(\mu,q^2)\right|^2\,+\,\left|C_{10A}(\mu)\right|^2\right)F_V^2(q^2)\,+\,\left(\frac{2\hat{m}_b}{\hat{s}}\right)^2\left|C_{7\gamma}(\mu)\,\bar{F}_{TV}(q^2)\right|^2$$
$$+\,\frac{4\hat{m}_b}{\hat{s}}\,F_V(q^2)\,Re\left(C_{7\gamma}(\mu)\,\bar{F}_{TV}(q^2)\,C_{9V}^{eff\,*}(\mu,q^2)\right),$$

$$F_2\left(\hat{s}\right) = \left(\left|C_{9V}^{\rm eff}(q^2,\mu)\right|^2\,+\,\left|C_{10A}(\mu)\right|^2\right)F_A^2(q^2)\,+\,\left(\frac{2\hat{m}_b}{\hat{s}}\right)^2\left|C_{7\gamma}(\mu)\,\bar{F}_{TA}(q^2)\right|^2$$
$$+\,\frac{4\hat{m}_b}{\hat{s}}\,F_A(q^2)\,Re\left(C_{7\gamma}(\mu)\,\bar{F}_{TA}(q^2)\,C_{9V}^{eff\,*}(\mu,q^2)\right).$$

Emission of the photon from valence quarks or FCNC vertex *(DE component)*

$$\frac{d^2\Gamma^{(2)}}{d\hat{s}\,d\hat{t}} = \frac{G_F^2\,\alpha_{em}^3\,M_1^5}{2^{10}\,\pi^4}\,\left|V_{tb}\,V_{tq}^*\right|^2\left(\frac{8\,f_{B_q}}{M_B}\right)^2\hat{m}_l^2\,\left|C_{10A}(\mu)\right|^2\left[\frac{\hat{s}\,+\,x^2/2}{(\hat{u}\,-\,\hat{m}_l^2)(\hat{t}\,-\,\hat{m}_l^2)}\,-\,\left(\frac{x\,\hat{m}_l}{(\hat{u}\,-\,\hat{m}_l^2)\,(\hat{t}\,-\,\hat{m}_l^2)}\right)^2\right] \qquad (6.2)$$

Bremsstrahlung

$$\frac{d^2\Gamma^{(12)}}{d\hat{s}\,d\hat{t}} = -\frac{G_F^2\,\alpha_{em}^3\,M_1^5}{2^{10}\,\pi^4}\,\left|V_{tb}\,V_{tq}^*\right|^2\,\frac{16\,f_{B_q}}{M_B}\,\hat{m}_l^2\,\frac{x^2}{(\hat{u}\,-\,\hat{m}_l^2)(\hat{t}\,-\,\hat{m}_{l34}^2)} \qquad (6.3)$$
$$\times\left[\frac{2\,x\,\hat{m}_b}{\hat{s}}\,Re\left(C_{10A}^*(\mu)C_{7\gamma}(\mu)\bar{F}_{TV}(q^2,0)\right)\,+\,x\,F_V(q^2)\,Re\left(C_{10A}^*(\mu)C_{9V}^{\rm eff}(\mu,q^2)\right)+\,\xi(\hat{s},\hat{t})\,F_A(q^2)\,\left|C_{10A}(\mu)\right|^2\right].$$

Interference

Melikhov and Nikitin, Phys. Rev. D 70 (2004) 114028
Kozachuk, Melikhov and Nikitin, Phys. Rev. D 97 (2018) 053007
Guadagnoli, Melikhov and Reboud, Phys.Lett.B 760 (2016) 442-447

Comparison among different FF computations in terms of BR

By focusing on the DE-only component of BR(Bs → $\mu\mu\gamma$) @ high-q2:

$\mathcal{B}(B_s^0 \to \mu^+\mu^-\gamma)[4.2\ \text{GeV}, m_{B_s^0}]$	
GNSV	$(1.63 \pm 0.80) \times 10^{-10}$
KMN [6]	$(1.83 \pm 0.69) \times 10^{-10}$
JPZ [7]	$(1.90 \pm 0.53) \times 10^{-9}$

Guadagnoli et al, JHEP '23 (2303.02174)

Comparison among different FF computations in terms of BR

By focusing on the DE-only component of BR(Bs → $\mu\mu\gamma$) @ high-q2:

$\mathcal{B}(B_s^0 \to \mu^+\mu^-\gamma)[4.2\text{ GeV}, m_{B_s^0}]$	
GNSV	$(1.63 \pm 0.80) \times 10^{-10}$
KMN [6]	$(1.83 \pm 0.69) \times 10^{-10}$
JPZ [7]	$(1.90 \pm 0.53) \times 10^{-9}$

Guadagnoli et al, JHEP '23 (2303.02174)

Comparison with lattice results:

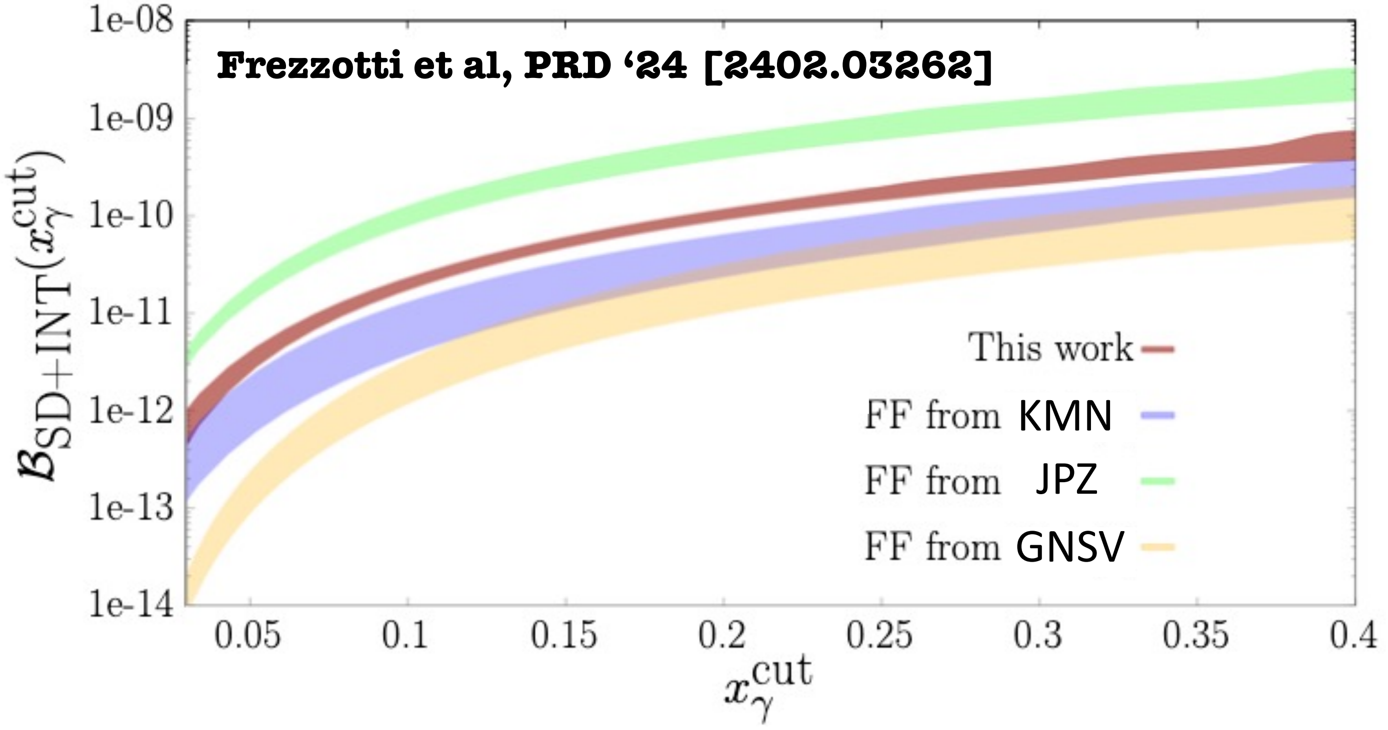

Integrated BR: BR × 10^{10} = $5.3(1.7)$

Comparison among different FF computations in terms of BR

By focusing on the DE-only component of BR(Bs → $\mu\mu\gamma$) @ high-q2:

$\mathcal{B}(B_s^0 \to \mu^+\mu^-\gamma)[4.2\ \text{GeV}, m_{B_s^0}]$	
GNSV	$(1.63 \pm 0.80) \times 10^{-10}$
KMN [6]	$(1.83 \pm 0.69) \times 10^{-10}$
JPZ [7]	$(1.90 \pm 0.53) \times 10^{-9}$

Guadagnoli et al, JHEP '23 (2303.02174)

Comparison with lattice results:

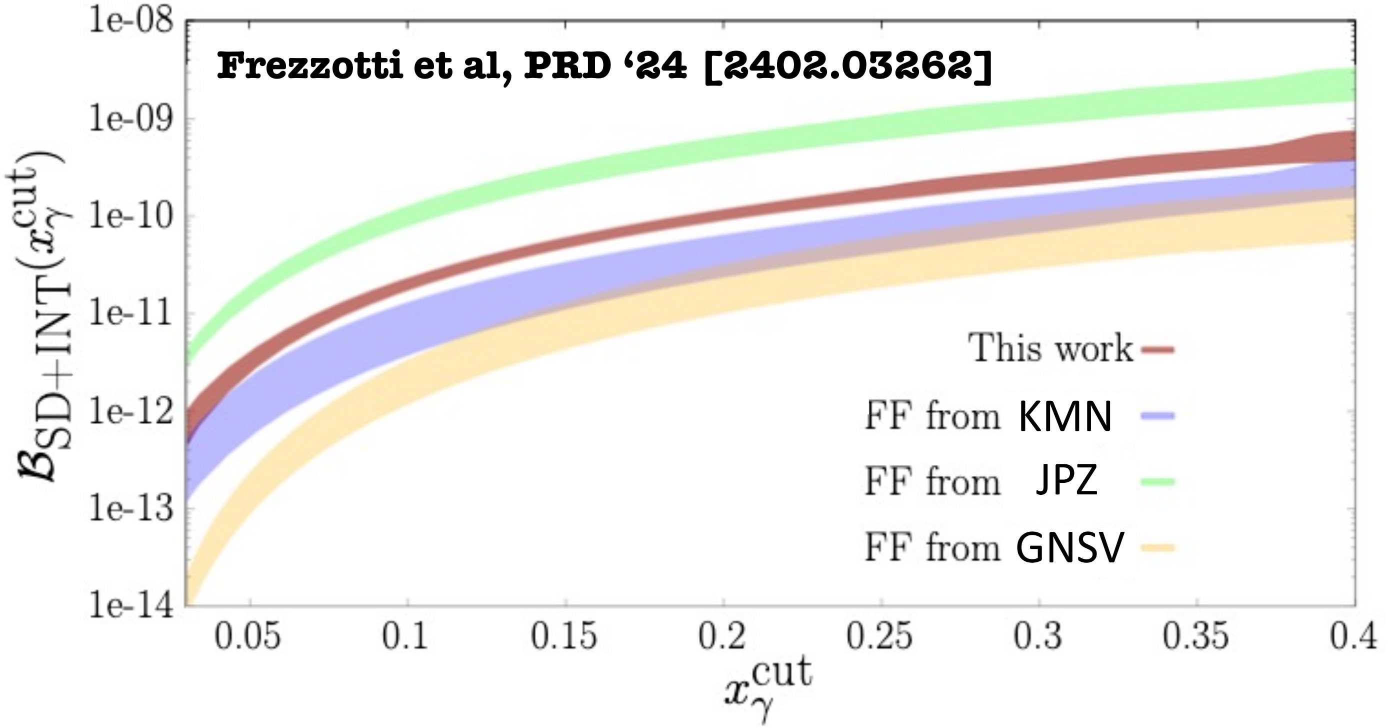

Integrated BR: BR × 10^{10} = $5.3(1.7)$

Differences @ (more or less) 2σ level despite the differences in the FFs values

Comparison among different FF computations in terms of BR

By focusing on the DE-only component of BR(Bs → $\mu\mu\gamma$) @ high-q2:

$\mathcal{B}(B_s^0 \to \mu^+\mu^-\gamma)[4.2\ \text{GeV}, m_{B_s^0}]$	
GNSV	$(1.63 \pm 0.80) \times 10^{-10}$
KMN [6]	$(1.83 \pm 0.69) \times 10^{-10}$
JPZ [7]	$(1.90 \pm 0.53) \times 10^{-9}$

Guadagnoli et al, JHEP '23 (2303.02174)

Comparison with lattice results:

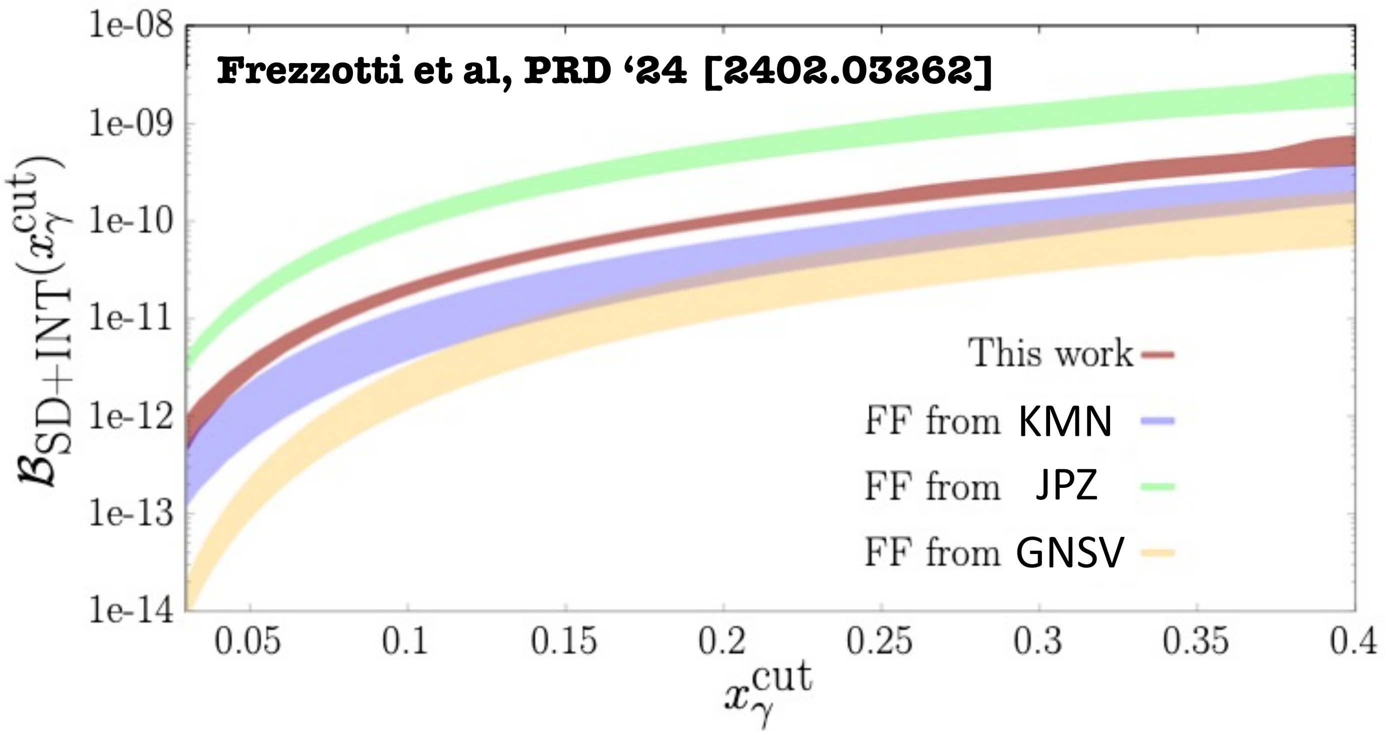

Integrated BR: BR × 10^{10} = $5.3(1.7)$

Differences @ (more or less) 2σ level despite the differences in the FFs values

Theor. issue to be further investigated: large uncertainties due to charmonia !

Brief recap of the GNSV procedure within the SM

To summarize: the GNSV procedure is based on a HQET scaling of FFs parameters from the Ds-sector to the Bs-sector, starting from LQCD data available for the Ds-sector @ high-q2.

This procedure must be applied @ high-q2,
***since only there an expansion of the FFs in terms of* P**
or PP *expressions is completely reliable!*

Brief recap of the GNSV procedure within the SM

To summarize: the GNSV procedure is based on a HQET scaling of FFs parameters from the Ds-sector to the Bs-sector, starting from LQCD data available for the Ds-sector @ high-q2.

→ ***This procedure must be applied @ high-q2, since only there an expansion of the FFs in terms of $\mathbb{P}$ or $\mathbb{PP}$ expressions is completely reliable!***

Important remarks for the future:

- **new lattice data have come out in the recent past/should come out in the near future, for sure for the D_s-sector (hopefully also in the Bs-sector):**
  - **Frezzotti et al., PRD '23 [2306.05904]** → *synthetic data available*
  - **Giusti et al., PRD '23 [2302.01298] and arXiv:2505.11757** → *methodological proposals*
  - **...**
- **The GNSV procedure can be used as a useful framework to develop «global analyses» of Ds → γ and/or Bs → γ data! The results obtained in Frezzotti et al, PRD '24 [2402.03262] are a fundamental benchmark to compare with.**

Brief recap of the GNSV procedure within the SM

To summarize: the GNSV procedure is based on a HQET scaling of FFs parameters from the Ds-sector to the Bs-sector, starting from LQCD data available for the Ds-sector @ high-q2.

→ ***This procedure must be applied @ high-q2,***
since only there an expansion of the FFs in terms of $\mathbb{P}$
or $\mathbb{PP}$ expressions is completely reliable!

Important remarks for the future:

- **new lattice data have come out in the recent past/should come out in the near future, for sure for the D_s-sector (hopefully also in the Bs-sector):**
  - **Frezzotti et al., PRD '23 [2306.05904]** → *synthetic data available*
  - **Giusti et al., PRD '23 [2302.01298] and arXiv:2505.11757** → *methodological proposals*
  - **...**
- **The GNSV procedure can be used as a useful framework to develop «global analyses» of Ds → ɣ and/or Bs → ɣ data! The results obtained in Frezzotti et al, PRD '24 [2402.03262] are a fundamental benchmark to compare with.**

We need to improve as much as possible the precision from the theoretical side …

Brief recap of the GNSV procedure within the SM

To summarize: the GNSV procedure is based on a HQET scaling of FFs parameters from the Ds-sector to the Bs-sector, starting from LQCD data available for the Ds-sector @ high-q2.

This procedure must be applied @ high-q2,
***since only there an expansion of the FFs in terms of* P**
or* PP *expressions is completely reliable!

Important remarks for the future:

- **new lattice data have come out in the recent past/should come out in the near future, for sure for the D_s-sector (hopefully also in the Bs-sector):**
  - **Frezzotti et al., PRD '23 [2306.05904]** → *synthetic data available*
  - **Giusti et al., PRD '23 [2302.01298] and arXiv:2505.11757** → *methodological proposals*
  - **...**
- **The GNSV procedure can be used as a useful framework to develop «global analyses» of Ds → ɣ and/or Bs → ɣ data! The results obtained in Frezzotti et al, PRD '24 [2402.03262] are a fundamental benchmark to compare with.**

We need to improve as much as possible the precision from the theoretical side …

… since many progresses on the experimental side are going on! ☺

Method I: measure Bs → $\mu\mu\gamma$ with photon reconstruction

Pro: **Sensitive to low-q2 region, therefore, to larger set of Wilson coefficients**

Con: **Photon reconstruction worsen the resolution**

Method I: measure Bs → $\mu\mu\gamma$ with photon reconstruction

Pro: Sensitive to low-q2 region, therefore, to larger set of Wilson coefficients

Con: Photon reconstruction worsen the resolution

Three q^2 regions:

- Bin I: low-q^2 →
- Bin II: middle-q^2 →
- Bin III: high-q^2 →

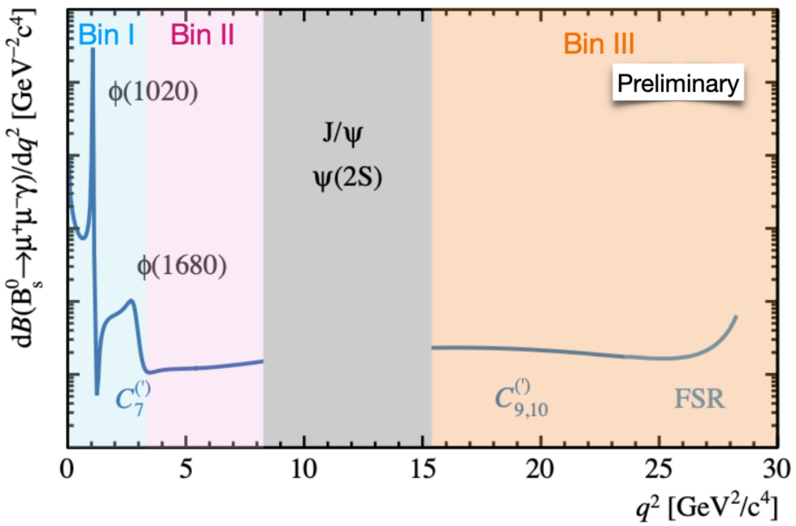

Phys.Rev.D70(2004)114028

CERN-THESIS-2020-303

$E_\gamma > 50\text{MeV}/c^2$

FSR = final state radiation

Additionally, Bin I is also studied with a veto on the ϕ-resonance mass:

$m(\mu^+\mu^-)$ = [989.6, 1073.4]MeV/c²

Bin I ϕ-veto: low-q^2 without ϕ region

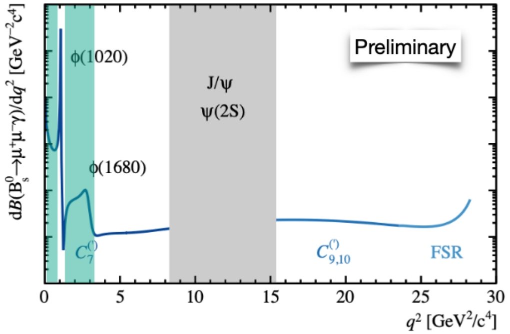

q^2 bin	I	II	III
q^2 [GeV^2/c^4]	$[4\,m_\mu^2, 2.89]$	$[2.89, 8.29]$	$[15.37, m_{B_s^0}^2]$
$m(\mu^+\mu^-)$ [GeV/c^2]	$[2\,m_\mu, 1.70]$	$[1.70, 2.88]$	$[3.92, m_{B_s^0}]$
$10^{10}\times\mathcal{B}(B_s^0\to\mu^+\mu^-\gamma)$ [8]	82 ± 15	2.54 ± 0.34	9.1 ± 1.1
Fraction of $B_s^0\to\mu^+\mu^-\gamma$	87%	2.7%	9.8%

Irene Bachiller - Search for the $B_s^0\to\mu^+\mu^-\gamma$ decay at LHCb 9

I. Bachiller, presentation @ «Workshop on radiative leptonic B decays», Marseille 2024

Method I: measure Bs → $\mu\mu\gamma$ with photon reconstruction

Pro: Sensitive to low-q2 region, therefore, to larger set of Wilson coefficients

Con: Photon reconstruction worsen the resolution

Three q² regions:

- Bin I: low-q² →
- Bin II: middle-q² →
- Bin III: high-q² →

Additionally, Bin I is also studied with a veto on the ϕ-resonance mass:

$m(\mu^+\mu^-)$ = [989.6, 1073.4]MeV/c²

Bin I ϕ-veto: low-q² without ϕ region

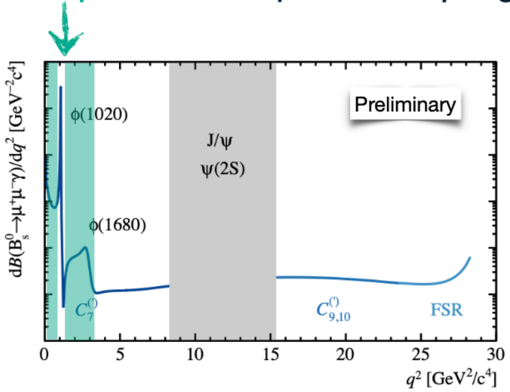

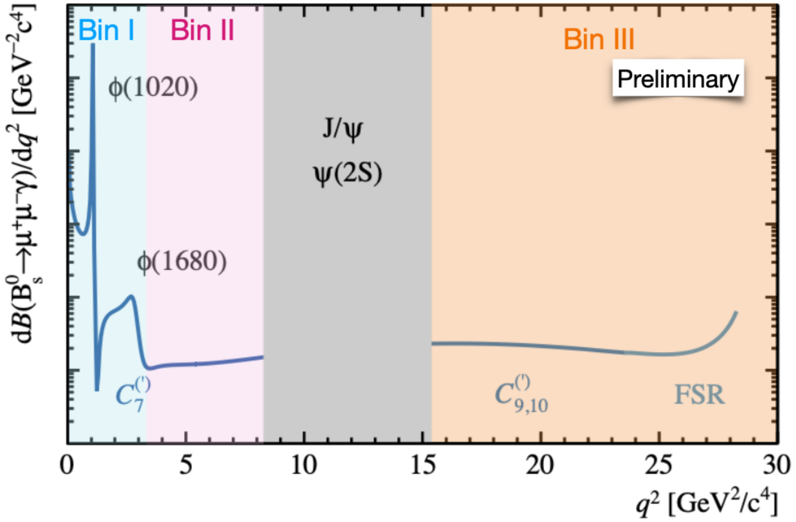

Phys.Rev.D70(2004)114028

CERN-THESIS-2020-303

$E_\gamma > 50\text{MeV}/c^2$

FSR = final state radiation

q^2 bin	I	II	III
q^2 [GeV²/c⁴]	$[4\,m_\mu^2, 2.89]$	$[2.89, 8.29]$	$[15.37, m_{B_s^0}^2]$
$m(\mu^+\mu^-)$ [GeV/c²]	$[2\,m_\mu, 1.70]$	$[1.70, 2.88]$	$[3.92, m_{B_s^0}]$
$10^{10}\times\mathcal{B}(B_s^0\to\mu^+\mu^-\gamma)$ [8]	82 ± 15	2.54 ± 0.34	9.1 ± 1.1
Fraction of $B_s^0\to\mu^+\mu^-\gamma$	87%	2.7%	9.8%

Irene Bachiller - Search for the $B_s^0\to\mu^+\mu^-\gamma$ decay at LHCb 9

Unfortunately, the measured BR is not statistically significant in any of the three regions…

I. Bachiller, presentation @ «Workshop on radiative leptonic B decays», Marseille 2024

Method I: measure Bs → $\mu\mu\gamma$ with photon reconstruction

Pro: Sensitive to low-q2 region, therefore, to larger set of Wilson coefficients

Con: Photon reconstruction worsen the resolution

Three q^2 regions:

- Bin I: low-q^2 →
- Bin II: middle-q^2 →
- Bin III: high-q^2 →

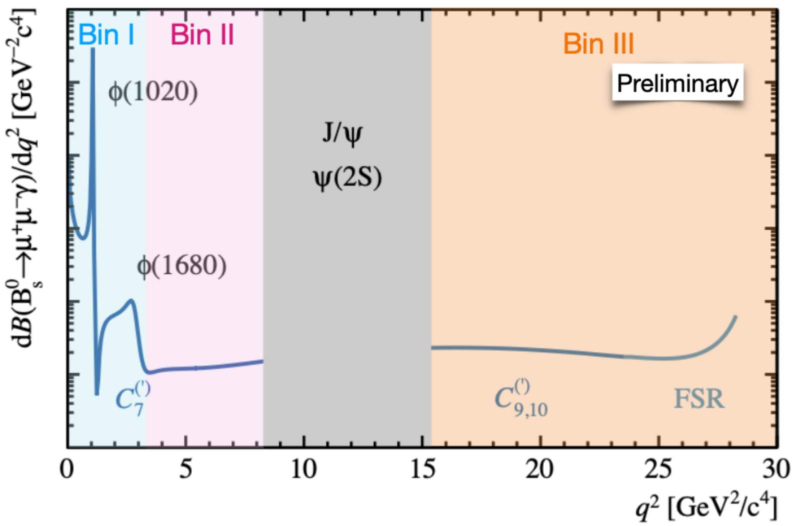

Phys.Rev.D70(2004)114028

CERN-THESIS-2020-303

$E_\gamma > 50\text{MeV}/c^2$

FSR = final state radiation

Additionally, Bin I is also studied with a veto on the ϕ-resonance mass:

$m(\mu^+\mu^-) = [989.6, 1073.4]\text{MeV}/c^2$

Bin I ϕ-veto: low-q^2 without ϕ region

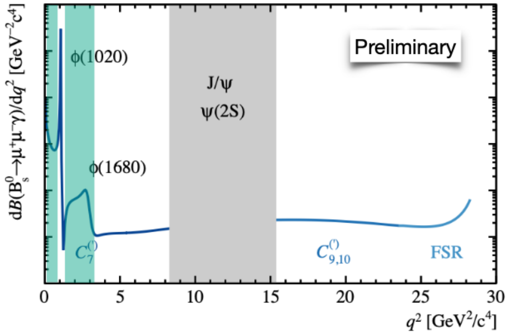

q^2 bin	I	II	III
q^2 [GeV^2/c^4]	$[4\,m_\mu^2, 2.89]$	$[2.89, 8.29]$	$[15.37, m_{B_s^0}^2]$
$m(\mu^+\mu^-)$ [GeV/c^2]	$[2\,m_\mu, 1.70]$	$[1.70, 2.88]$	$[3.92, m_{B_s^0}]$
$10^{10}\times\mathcal{B}(B_s^0\to\mu^+\mu^-\gamma)$ [8]	82 ± 15	2.54 ± 0.34	9.1 ± 1.1
Fraction of $B_s^0\to\mu^+\mu^-\gamma$	87%	2.7%	9.8%

Irene Bachiller - Search for the $B_s^0\to\mu^+\mu^-\gamma$ decay at LHCb 9

Unfortunately, the measured BR is not statistically significant in any of the three regions…

Upper limits on BR in the regions I, II and III (see next slides)

I. Bachiller, presentation @ «Workshop on radiative leptonic B decays», Marseille 2024

Method II: measure Bs → μμɣ without photon reconstruction

The basic idea is to reconstruct the radiative signal from the non-radiative counterpart, namely

$$B_s^0 \to \mu^+\mu^-\gamma \text{ from } B_s^0 \to \mu^+\mu^-$$

Dettori, Guadagnoli, Reboud, Phys.Lett.B 768 (2017) 163-167

Method II: measure Bs → μμɣ without photon reconstruction

The basic idea is to reconstruct the radiative signal from the non-radiative counterpart, namely

$$B_s^0 \to \mu^+\mu^-\gamma \text{ from } B_s^0 \to \mu^+\mu^-$$

Dettori, Guadagnoli, Reboud, Phys.Lett.B 768 (2017) 163-167

How? Enlarging the dilepton invariant mass below the Bs-peak (it works IF the bkgs are well under control!)

The problem is in other words

$$\mathcal{B}(B_s^0 \to \mu^+\mu^- + n\gamma) \quad \textbf{VS} \quad \mathcal{B}(B_s^0 \to \mu^+\mu^-\gamma)$$

Method II: measure Bs → **$\mu\mu\gamma$** <u>without</u> photon reconstruction

The basic idea is to reconstruct the radiative signal from the non-radiative counterpart, namely

$$B_s^0 \to \mu^+\mu^-\gamma \textbf{ from } B_s^0 \to \mu^+\mu^-$$

Dettori, Guadagnoli, Reboud, Phys.Lett.B 768 (2017) 163-167

How? Enlarging the dilepton invariant mass below the Bs-peak
(it works <u>IF</u> the bkgs are well under control!)

The problem is in other words

$$\mathcal{B}(B_s^0 \to \mu^+\mu^- + n\gamma) \textbf{ VS } \mathcal{B}(B_s^0 \to \mu^+\mu^-\gamma)$$

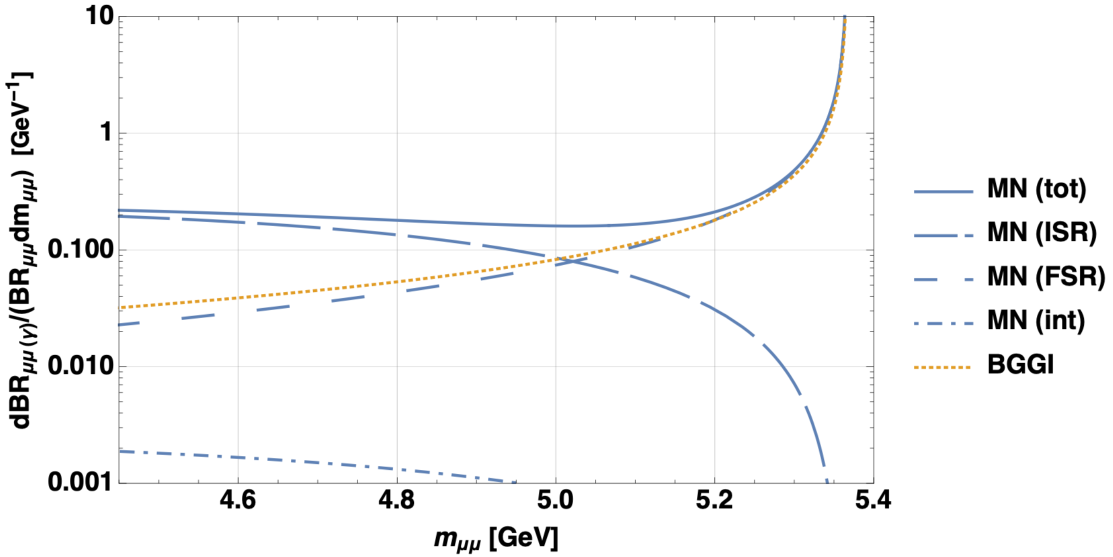

MN = Melikhov, Nikitin, PRD '04 [hep-ph/0410146]
BGGI = Buras, Girrbach, Guadagnoli, Isidori, EPJC '12 [1208.0934]

Method II: measure Bs → $\mu\mu\gamma$ without photon reconstruction

The basic idea is to reconstruct the radiative signal from the non-radiative counterpart, namely

$$B_s^0 \to \mu^+\mu^-\gamma \textbf{ from } B_s^0 \to \mu^+\mu^-$$

Dettori, Guadagnoli, Reboud, Phys.Lett.B 768 (2017) 163-167

How? Enlarging the dilepton invariant mass below the Bs-peak
(it works IF the bkgs are well under control!)

The problem is in other words

$$\mathcal{B}(B_s^0 \to \mu^+\mu^- + n\gamma) \textbf{ VS } \mathcal{B}(B_s^0 \to \mu^+\mu^-\gamma)$$

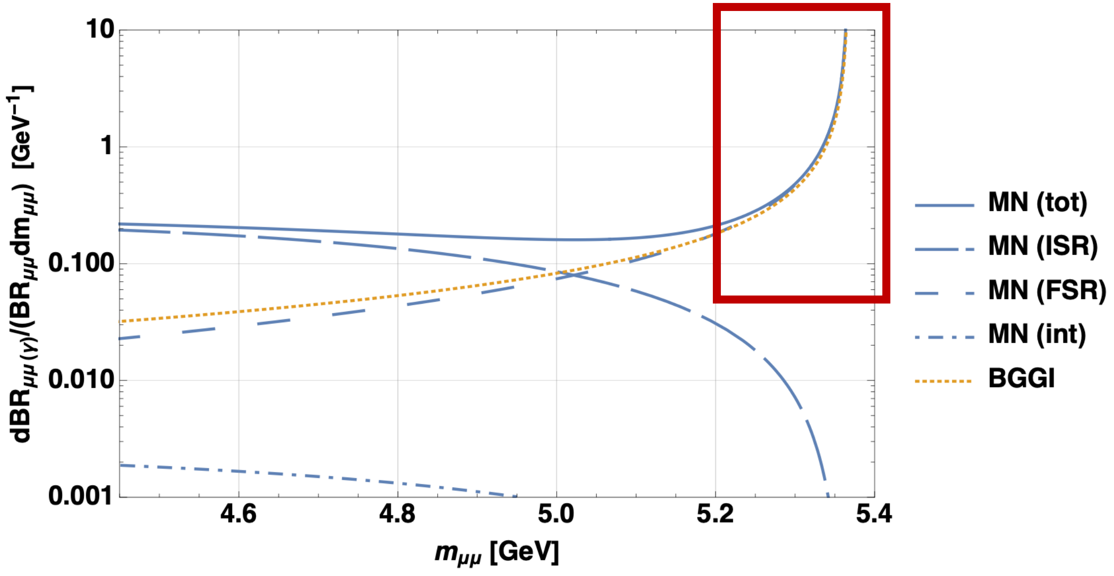

For very soft photons, the single-photon component of the former should be equal to the latter!

MN = Melikhov, Nikitin, PRD '04 [hep-ph/0410146]

BGGI = Buras, Girrbach, Guadagnoli, Isidori, EPJC '12 [1208.0934]

Method II: measure Bs → μμγ without photon reconstruction

$$\mathcal{B}(B_s^0 \to \mu^+\mu^-\gamma) < 2.0 \times 10^{-9} \quad \{ m_{\mu\mu} > 4.9\,\mathrm{GeV}/c^2 \}$$

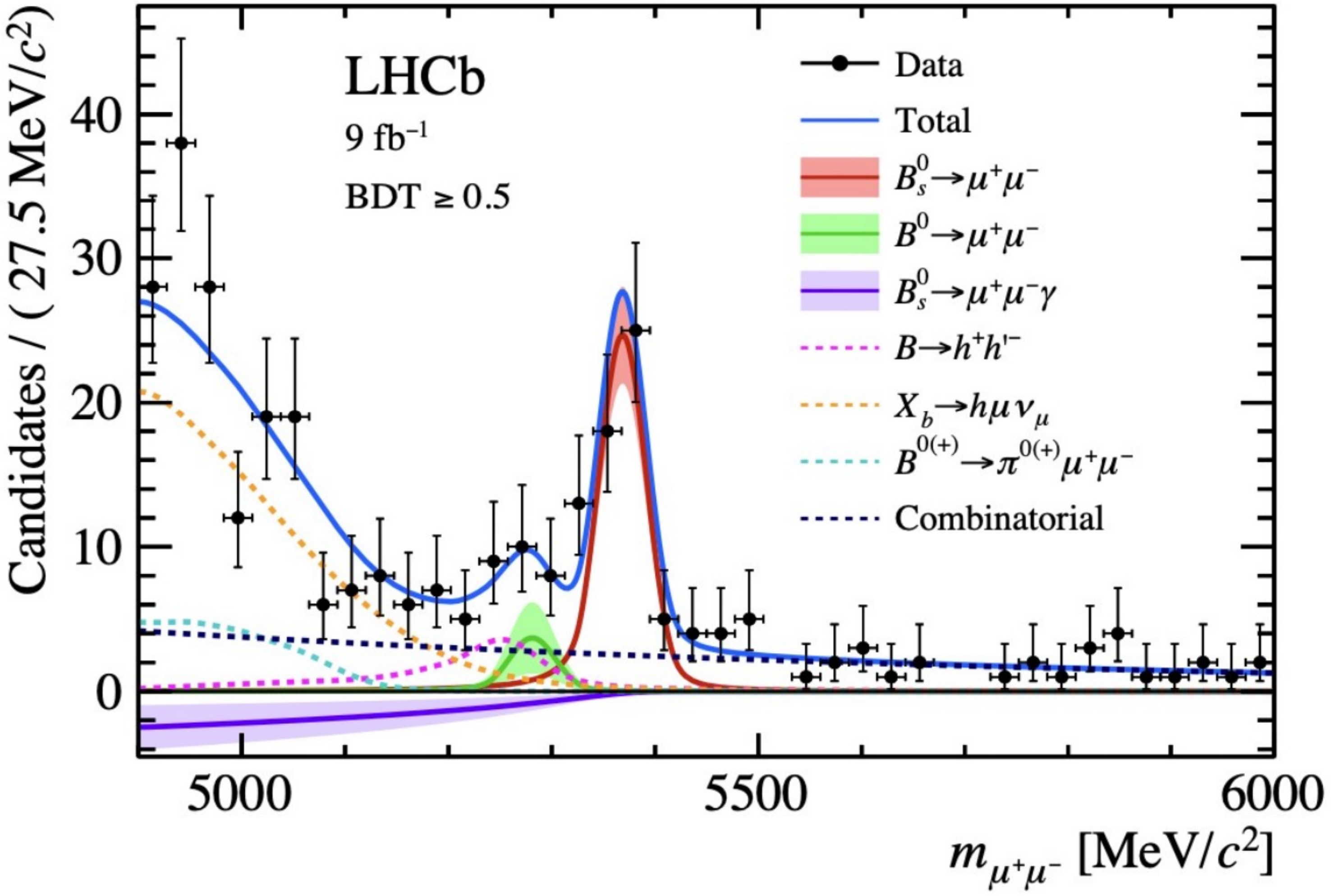

(from LHCb-PAPER-2021-007, LHCb-PAPER-2021-008)

Method II: measure **Bs → μμγ** without photon reconstruction

$$\mathcal{B}(B_s^0 \to \mu^+\mu^-\gamma) \; < \; 2.0 \times 10^{-9} \quad \left\{ m_{\mu\mu} > 4.9\,\mathrm{GeV}/c^2 \right\}$$

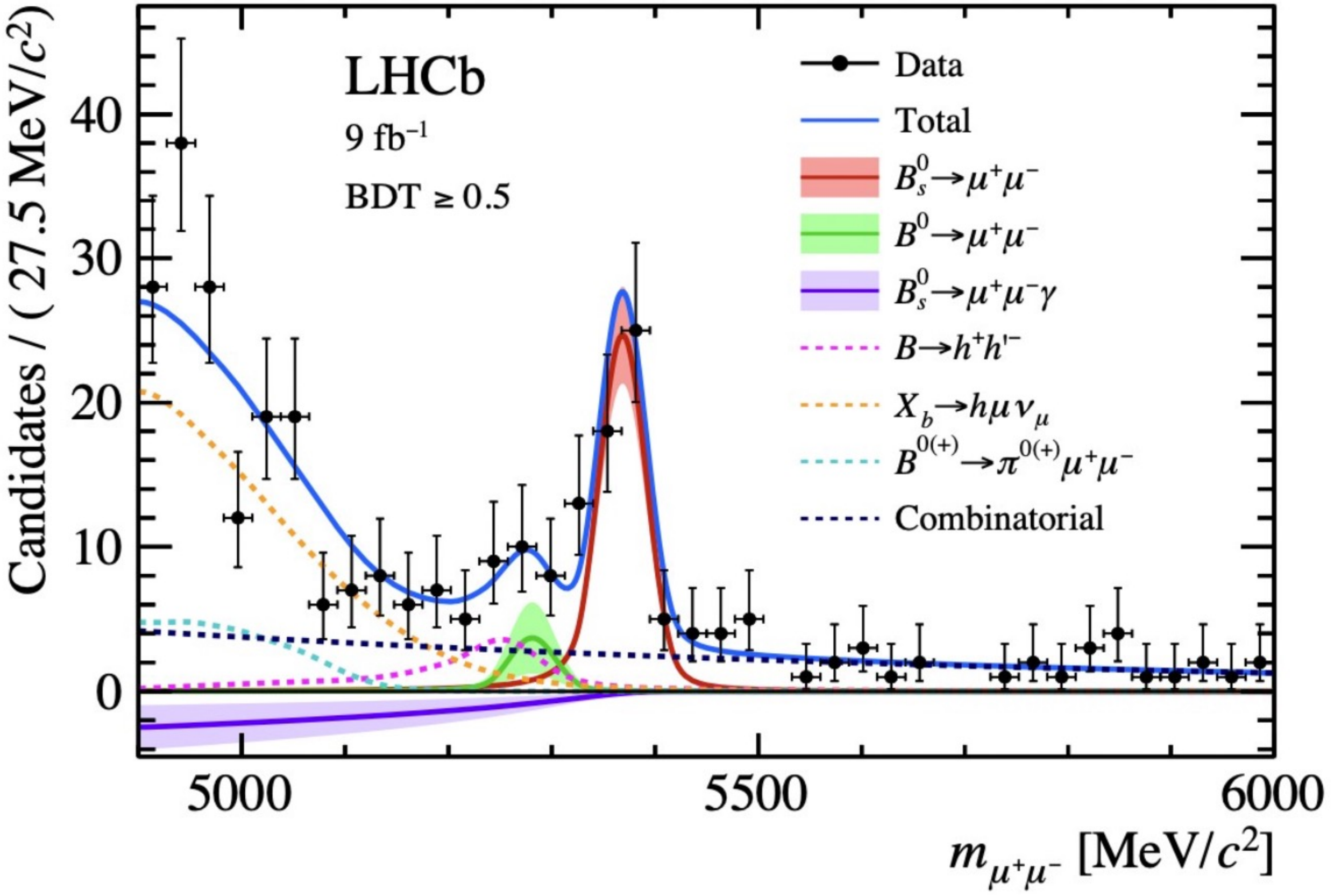

(from LHCb-PAPER-2021-007, LHCb-PAPER-2021-008)

Pros:

i) **No recontruction of the photon,** whose efficieny is inherently small

ii) **Measur. at high-q2, which is the best region for Lattice QCD** and is also the region least affected by resonances

iii) **Sensitivity to C_9, C_{10}**

Method II: measure **Bs → μμɣ** without photon reconstruction

$$\mathcal{B}(B_s^0 \to \mu^+\mu^-\gamma) < 2.0 \times 10^{-9} \quad \{ m_{\mu\mu} > 4.9\,\mathrm{GeV}/c^2 \}$$

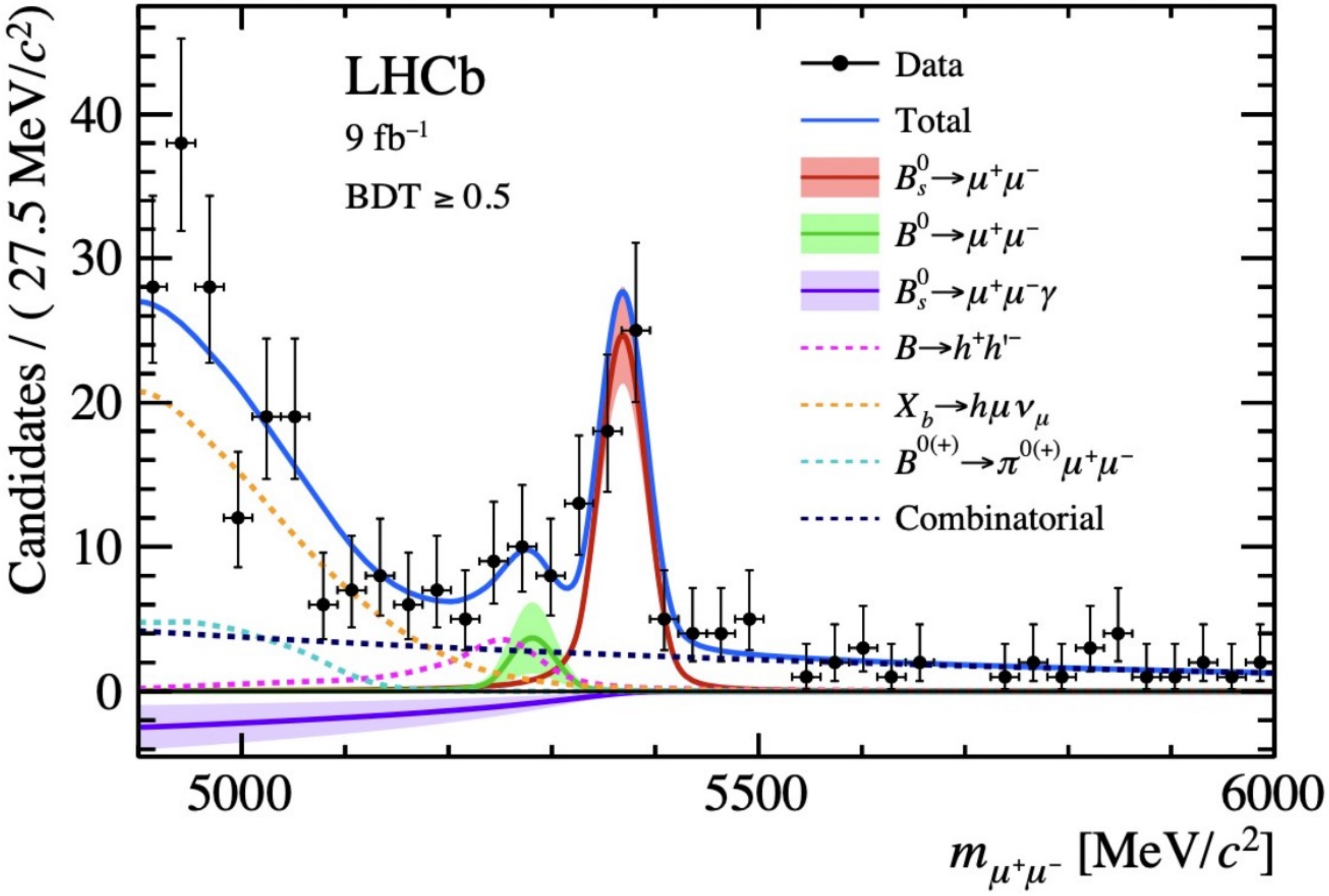

(from LHCb-PAPER-2021-007, LHCb-PAPER-2021-008)

Pros:

i) **No recontruction of the photon,** whose efficieny is inherently small

ii) **Measur. at high-q2, which is the best region for Lattice QCD** and is also the region least affected by resonances

iii) **Sensitivity to C_9, C_{10}**

Cons:

i) **Signal as a «shoulder»,** i.e. requires reliable estimation of all other «shoulders»

ii) **Difficult below $(4.2\ \mathrm{GeV})^2$**

iii) **Mass resolution crucial !!**

Summary of all (th. and exp.) results within the SM

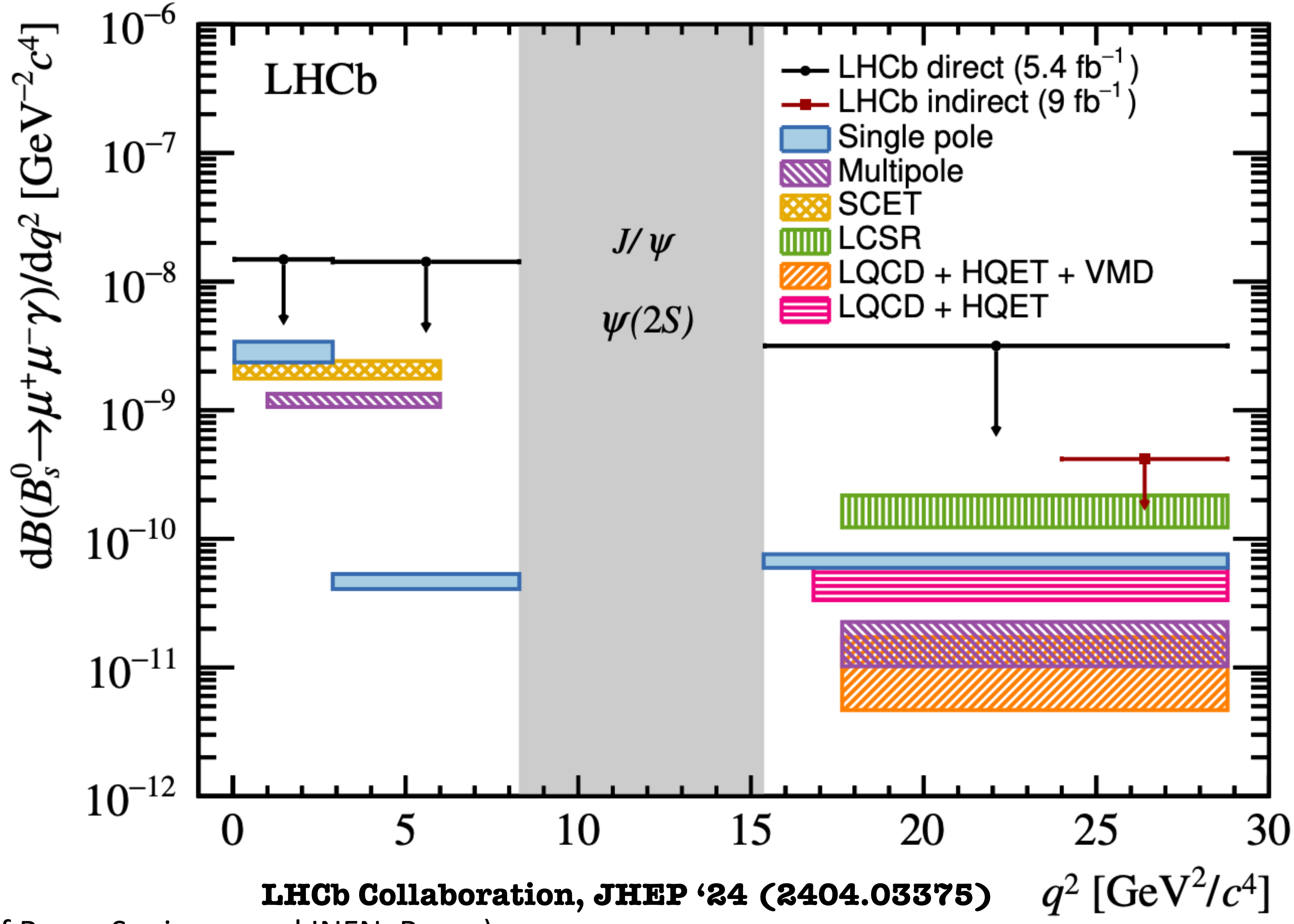

LHCb Collaboration, JHEP '24 (2404.03375)

Summary of all (th. and exp.) results within the SM

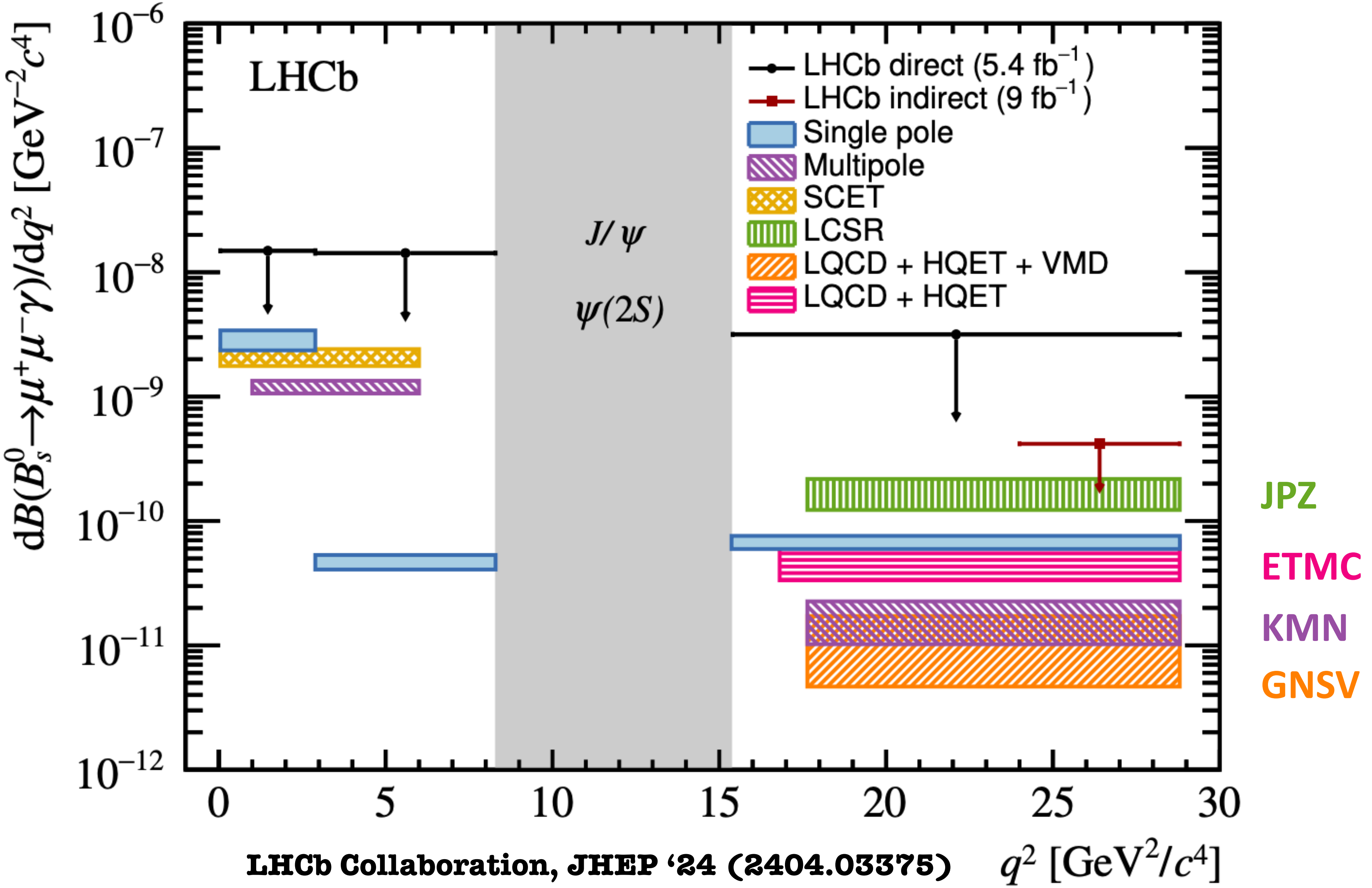

LHCb Collaboration, JHEP '24 (2404.03375)

Summary of all (th. and exp.) results within the SM

SCET computation at low-q2

BBW, JHEP '24 (2008.12494)

Single-pole parametrization

Guadagnoli, Reboud, Zwicky JHEP '17 (1708.02649)

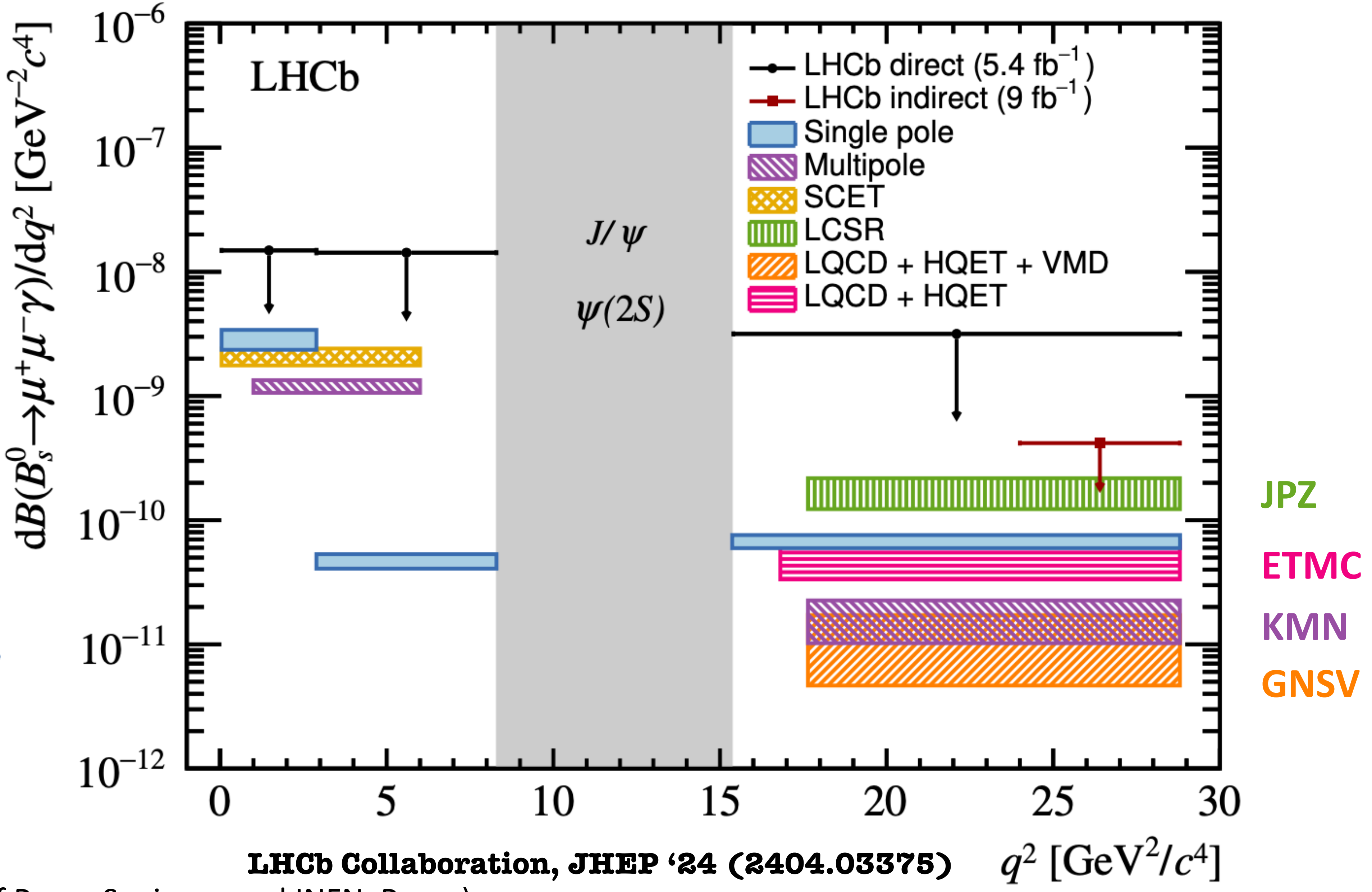

LHCb Collaboration, JHEP '24 (2404.03375)

Summary of all (th. and exp.) results within the SM

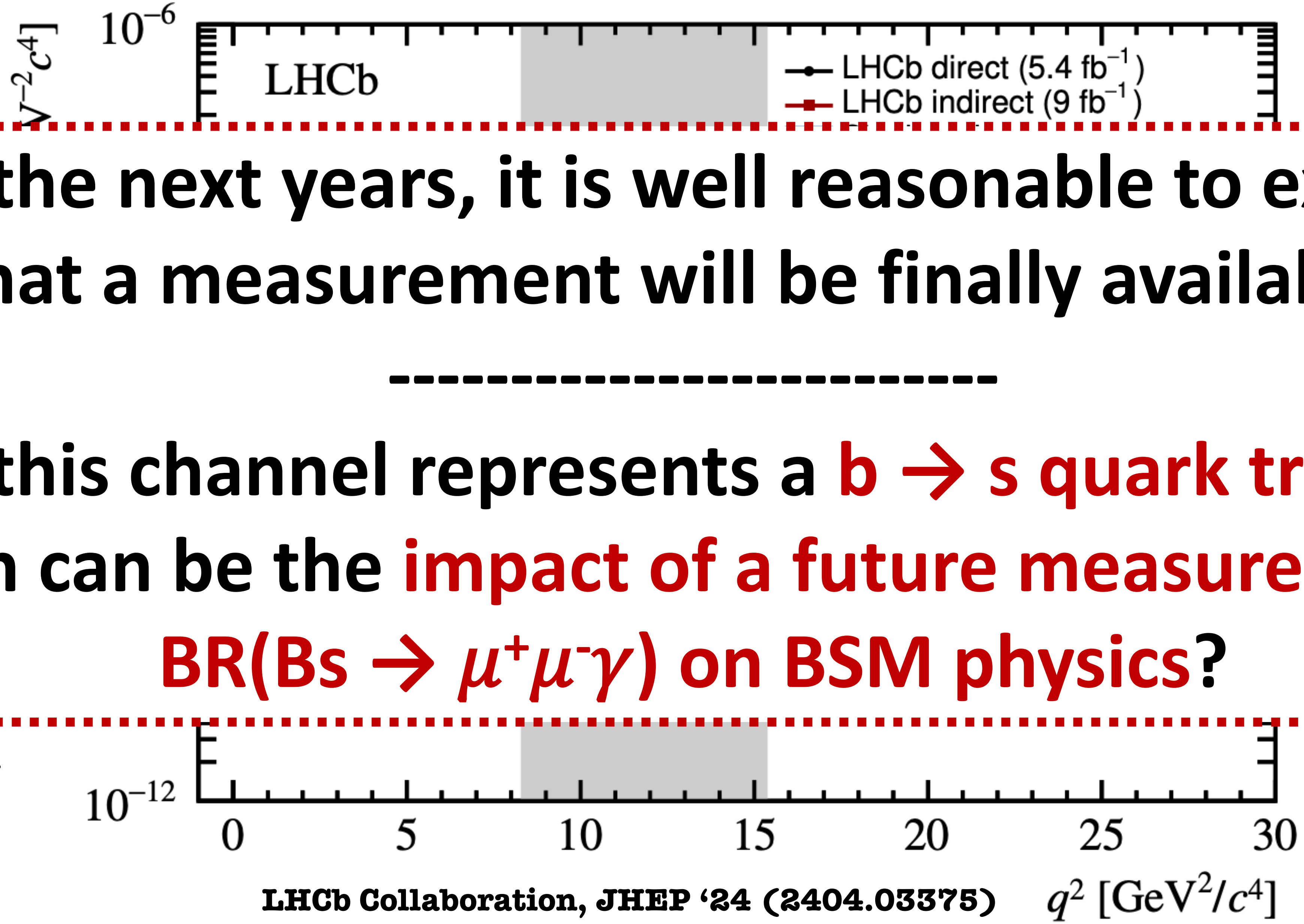

In the next years, it is well reasonable to expect that a measurement will be finally available !

Since this channel represents a b → s quark transition, which can be the impact of a future measurement of BR(Bs → $\mu^+\mu^-\gamma$) on BSM physics?

Guadagnoli, Reboud, Zwicky JHEP '17 (1708.02649)

LHCb Collaboration, JHEP '24 (2404.03375)

The relevance of $B_s \to \gamma$ beyond the SM

The $B_s \to \mu\mu\gamma$ channel can be used to study hypothetical New Physics (NP) effects affecting *b → s quark transition*. In fact, despite the disappearance of the R(K(*)) anomalies, we have several discrepancies among theory and experiments in semileptonic neutral-current *B* decays:

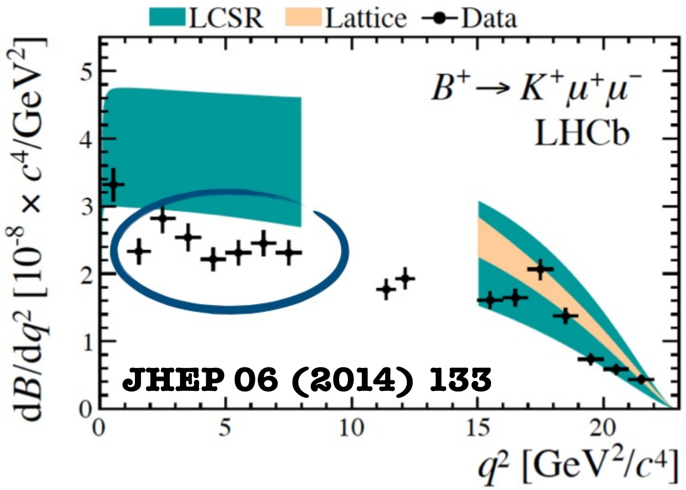

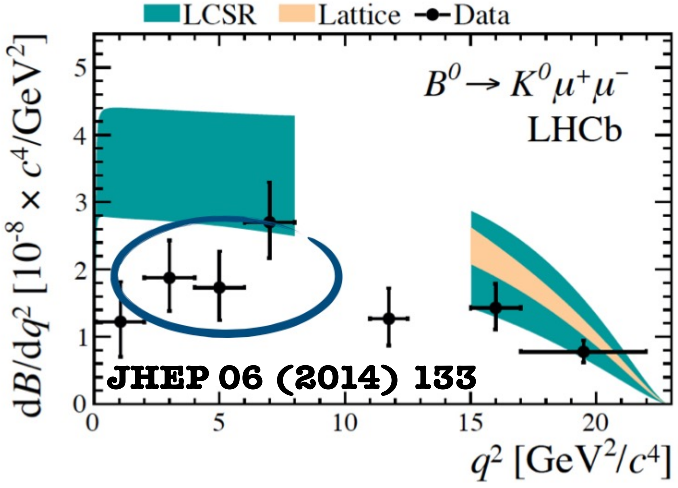

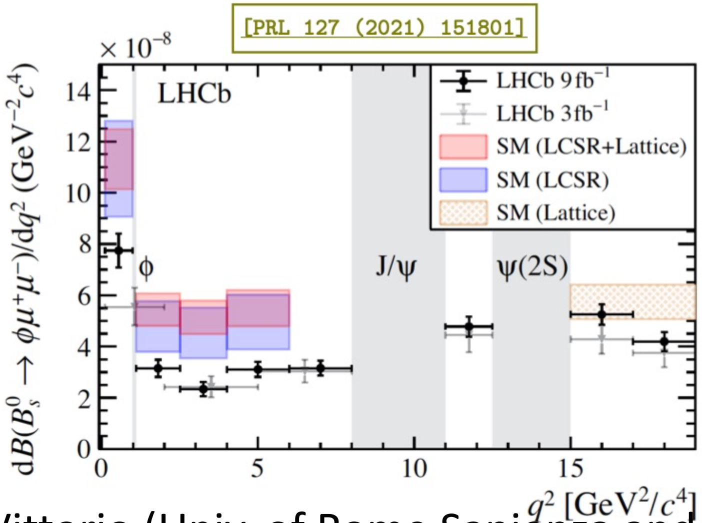

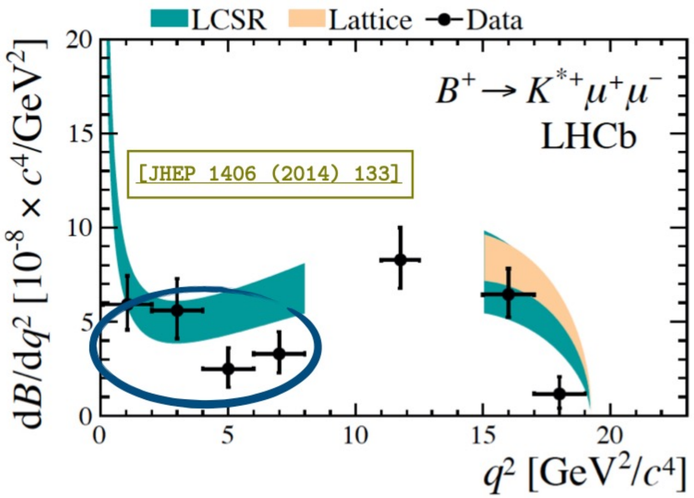

The relevance of $B_s \to \gamma$ beyond the SM

The $B_s \to \mu\mu\gamma$ channel can be used to study hypothetical New Physics (NP) effects affecting *b → s quark transition*. In fact, despite the disappearance of the R(K(*)) anomalies, we have several discrepancies among theory and experiments in semileptonic neutral-current *B* decays:

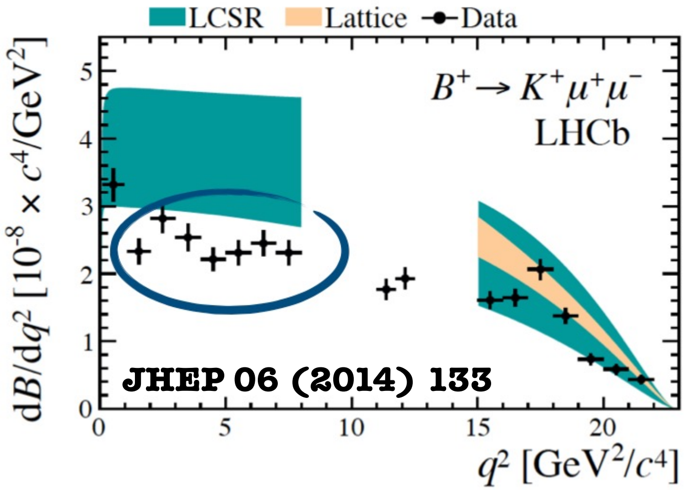

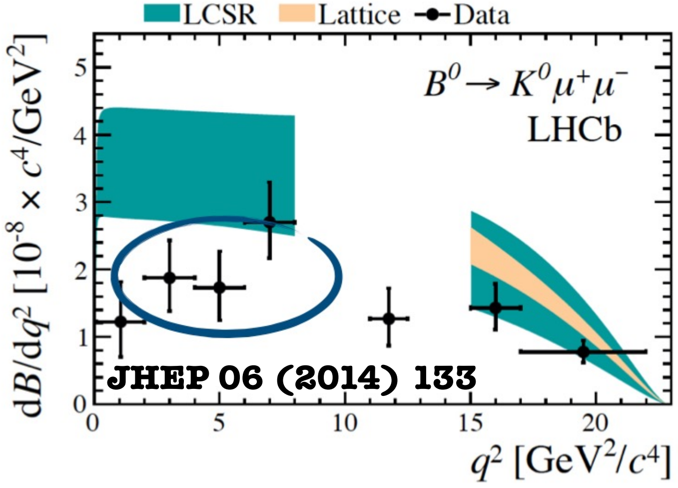

SM expectations seem to be *always above* experimental data …

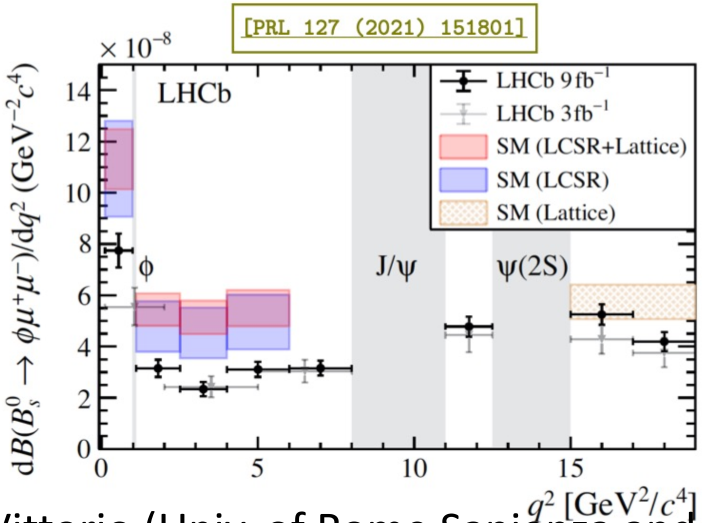

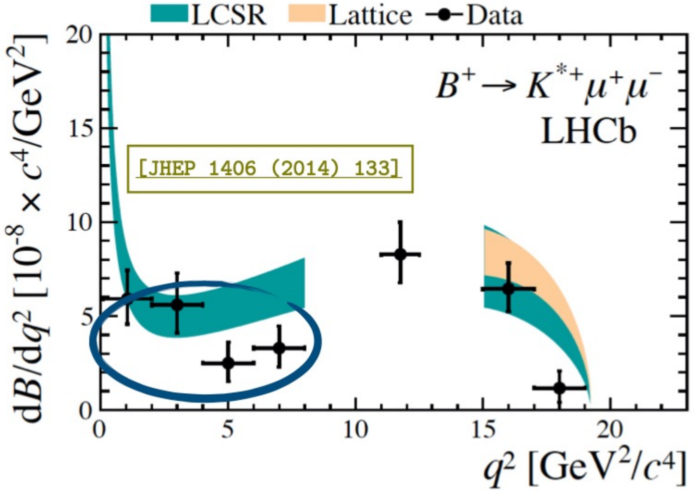

The relevance of $B_s \to \gamma$ beyond the SM

The $B_s \to \mu\mu\gamma$ channel can be used to study hypothetical New Physics (NP) effects affecting *b → s quark transition*. In fact, despite the disappearance of the R(K(*)) anomalies, we have several discrepancies among theory and experiments in semileptonic neutral-current *B* decays:

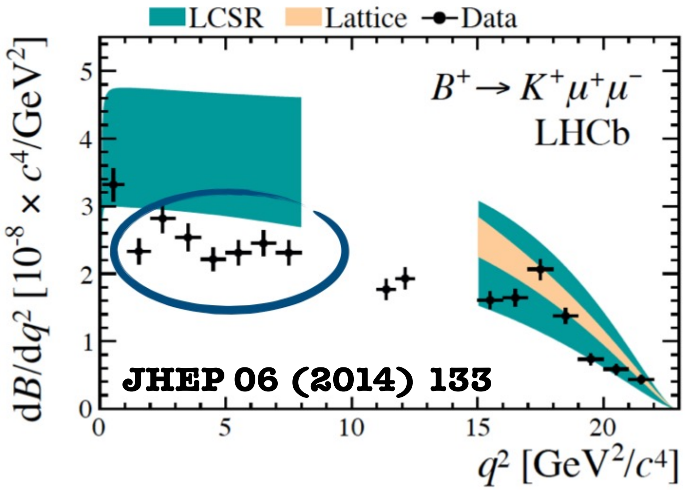

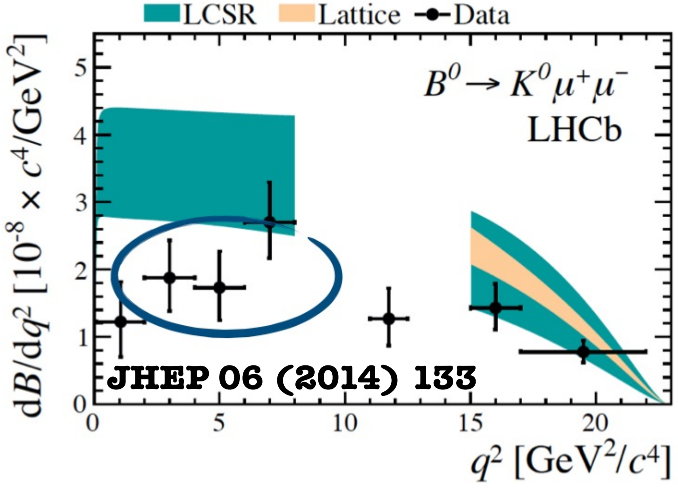

SM expectations seem to be *always above* experimental data …

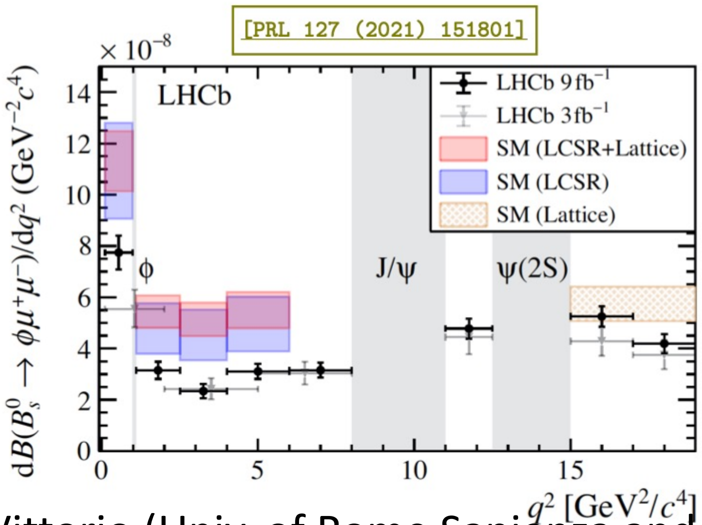

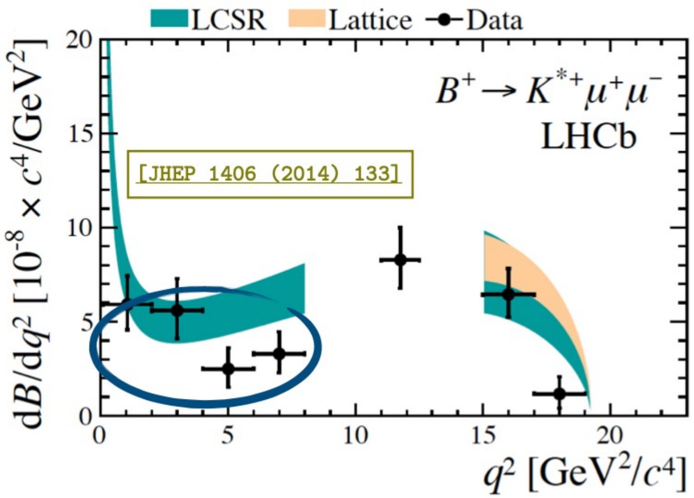

Important debate: is there really NP? Were the hadronic effects (namely long-distance ones) treated correctly ?

$B_s \to \mu\mu\gamma$ as a golden channel to study NP

KEY IDEA: **high-q2 observables are sensitive to the very same short-distance physics present in B \to K(*) decays, without being affected by the same long-distance effects !**

$B_s \to \mu\mu\gamma$ as a golden channel to study NP

<u>KEY IDEA:</u> high-q2 observables are sensitive to the very same short-distance physics present in B \to K(*) decays, without being affected by the same long-distance effects !

$B_s \to \mu\mu\gamma$ as a perfect candidate: if there is really NP in B \to K(*) decays, *i.e.* if there is really a NP contribution to C_9, this effect must influence as well the BR($B_s \to \mu\mu\gamma$) @ high-q2

$B_s \to \mu\mu\gamma$ as a golden channel to study NP

KEY IDEA: **high-q2 observables are sensitive to the very same short-distance physics present in B \to K(*) decays, without being affected by the same long-distance effects !**

$B_s \to \mu\mu\gamma$ as a perfect candidate: if there is really NP in B \to K(*) decays, *i.e.* if there is really a NP contribution to C_9, this effect must influence as well the BR($B_s \to \mu\mu\gamma$) @ high-q2

However, we do not have a direct measurement of BR($B_s \to \mu\mu\gamma$) @ high-q2 at present …

Thus, the best that we can do at present is a sensitivity study !

$B_s \to \mu\mu\gamma$ as a golden channel to study NP

Main ingredients of our sensitivity study:

1. ***Identification of NP benchmarks***
   from semileptonic neutral-current B decays:

NP shift		ℓ-specific + ℓ-univ. parts
δC_k^{bsee}	$\equiv$	$\delta C_k^{(e)} + \delta C_k^{u(e,\mu)}$
$\delta C_k^{bs\mu\mu}$	$\equiv$	$\delta C_k^{(\mu)} + \delta C_k^{u(e,\mu)}$

$(k = 9,\ 10)$

$B_s \to \mu\mu\gamma$ as a golden channel to study NP

Main ingredients of our sensitivity study:

1. ***Identification of NP benchmarks***
   from semileptonic neutral-current B decays:

NP shift		ℓ-specific + ℓ-univ. parts
δC_k^{bsee}	$\equiv$	$\delta C_k^{(e)} + \delta C_k^{u(e,\mu)}$
$\delta C_k^{bs\mu\mu}$	$\equiv$	$\delta C_k^{(\mu)} + \delta C_k^{u(e,\mu)}$

$(k = 9,\ 10)$

$$\left[\ \delta C_9^{(\ell)} = -\delta C_{10}^{(\ell)} \equiv \delta C_{LL}^{(\ell)}/2\ \right]$$

by fitting the data (see back-up slides for their list)

Scenario	Best-fit point	1σ Interval	$\sqrt{\chi^{2,\mathrm{SM}} - \chi^2}$
$(\delta C_9^{u(e,\mu)}, \delta C_{10}^{u(e,\mu)}) \in \mathbb{R}$	$(-0.88, +0.30)$	$([-1.08, -0.56], [0.15, 0.46])$	5.5
$\delta C_{LL}^{u(e,\mu)}/2 \in \mathbb{C}$	$-0.70 - 1.36i$	$[-1.00, -0.54] + i[-1.77, -0.54]$	5.8
$\delta C_9^{u(e,\mu)} \in \mathbb{C}$	$-1.08 + 0.10i$	$[-1.31, -0.85] + i[-0.70, +0.85]$	6.4
$\delta C_{10}^{u(e,\mu)} \in \mathbb{C}$	$+0.68 + 1.40i$	$[+0.38, +1.00] + i[+0.69, +1.92]$	3.2

$B_s \to \mu\mu\gamma$ as a golden channel to study NP

Main ingredients of our sensitivity study:

1. ***Identification of NP benchmarks*** ***from semileptonic neutral-current B decays:***

NP shift		ℓ-specific + ℓ-univ. parts
δC_k^{bsee}	$\equiv$	$\delta C_k^{(e)} + \delta C_k^{u(e,\mu)}$
$\delta C_k^{bs\mu\mu}$	$\equiv$	$\delta C_k^{(\mu)} + \delta C_k^{u(e,\mu)}$

$(k = 9,\, 10)$

$$\left[\delta C_9^{(\ell)} = -\delta C_{10}^{(\ell)} \equiv \delta C_{LL}^{(\ell)}/2\right]$$

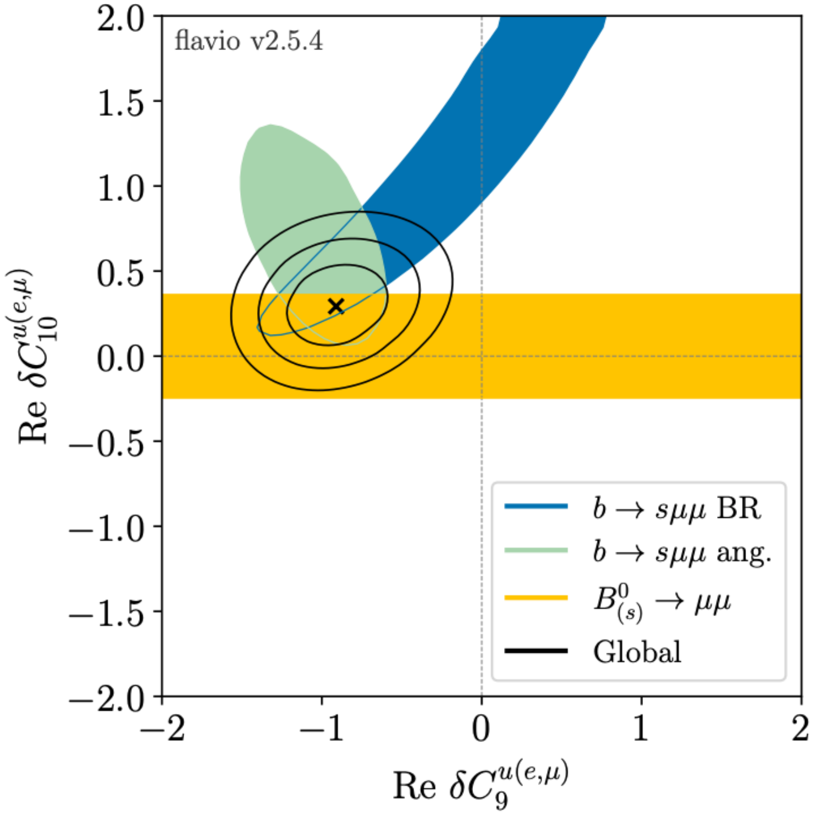

EXAMPLE

by fitting the data (see back-up slides for their list)

Scenario	Best-fit point	1σ Interval	$\sqrt{\chi^{2,\mathrm{SM}} - \chi^2}$
$(\delta C_9^{u(e,\mu)}, \delta C_{10}^{u(e,\mu)}) \in \mathbb{R}$	$(-0.88, +0.30)$	$([-1.08, -0.56], [0.15, 0.46])$	5.5
$\delta C_{LL}^{u(e,\mu)}/2 \in \mathbb{C}$	$-0.70 - 1.36i$	$[-1.00, -0.54] + i[-1.77, -0.54]$	5.8
$\delta C_9^{u(e,\mu)} \in \mathbb{C}$	$-1.08 + 0.10i$	$[-1.31, -0.85] + i[-0.70, +0.85]$	6.4
$\delta C_{10}^{u(e,\mu)} \in \mathbb{C}$	$+0.68 + 1.40i$	$[+0.38, +1.00] + i[+0.69, +1.92]$	3.2

$B_s \to \mu\mu\gamma$ as a golden channel to study NP

Main ingredients of our sensitivity study:

1. ***Identification of NP benchmarks***
   from semileptonic neutral-current B decays:

NP shift		ℓ-specific + ℓ-univ. parts
δC_k^{bsee}	$\equiv$	$\delta C_k^{(e)} + \delta C_k^{u(e,\mu)}$
$\delta C_k^{bs\mu\mu}$	$\equiv$	$\delta C_k^{(\mu)} + \delta C_k^{u(e,\mu)}$

$(k = 9,\, 10)$

$$\left[\, \delta C_9^{(\ell)} = -\delta C_{10}^{(\ell)} \equiv \delta C_{LL}^{(\ell)}/2 \,\right]$$

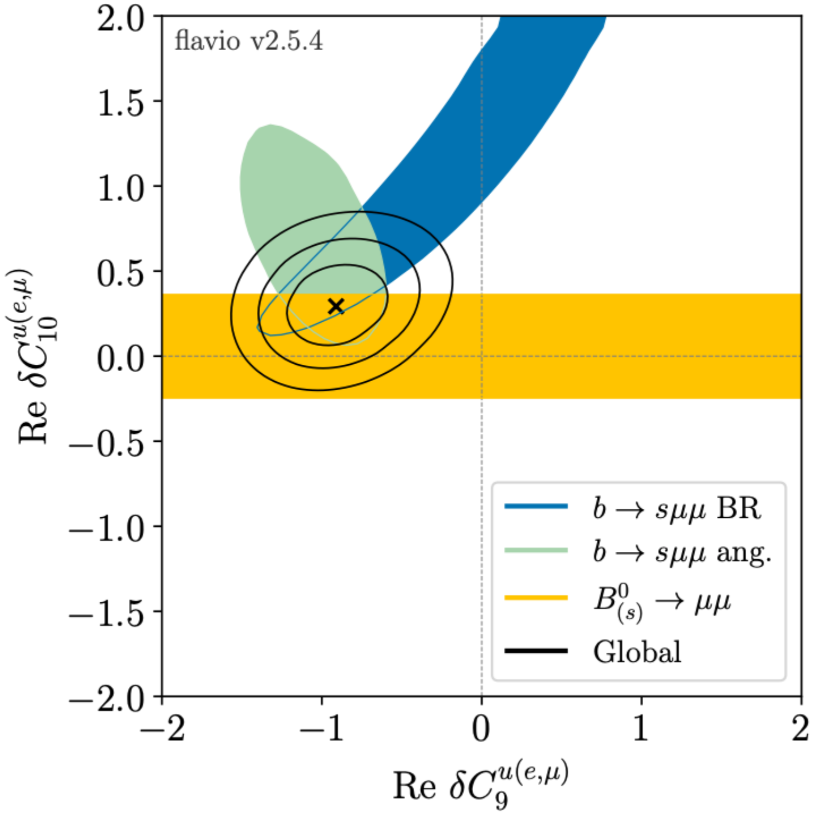

EXAMPLE

***REMARK*: we are computing these NP shifts assuming,**
as said before, that SM long-distance effects are negligible !!
(See also the global analyses in JHEP '23 [2212.10497], PRD '23 [2212.10516] …)

$B_s \to \mu\mu\gamma$ as a golden channel to study NP

Main ingredients of our sensitivity study:

2. ***Experimental uncertainties:* *we will assume that all the backgrounds are under control, i.e. that their uncertainties will eventually fall safely below the signal yield ("no-background" hypothesis).***

Thus, the Bs → μμγ-signal uncertainty will be dominated by the sheer amount of data collected

(Many effects to be taken into account: efficiencies, optimal choice of $(q_{min})^2$, …)

$B_s \to \mu\mu\gamma$ as a golden channel to study NP

Main ingredients of our sensitivity study:

2. ***Experimental uncertainties:* we will assume that all the backgrounds are under control, i.e. that their uncertainties will eventually fall safely below the signal yield ("no-background" hypothesis).**

> ***Thus, the Bs → μμγ-signal uncertainty***
> ***will be dominated by the sheer amount of data collected***

(Many effects to be taken into account: efficiencies, optimal choice of $(q_{min})^2$, …)

3. ***Theoretical uncertainties:***

- GNSV FFs with shrinked uncertainties, i.e. O(5%) errors, and KMN tensor FFs with O(20%) uncertainties

- <u>assumption</u>: broad charmonia play an entirely negligible role at high-q2

$B_s \to \mu\mu\gamma$ as a golden channel to study NP

Main ingredients of our sensitivity study:

2. ***Experimental uncertainties:* *we will assume that all the backgrounds are under control, i.e. that their uncertainties will eventually fall safely below the signal yield ("no-background" hypothesis).***

Thus, the Bs → μμγ-signal uncertainty
will be dominated by the sheer amount of data collected

(Many effects to be taken into account: efficiencies, optimal choice of $(q_{min})^2$, …)

3. ***Theoretical uncertainties:***
   - ***GNSV FFs with shrinked uncertainties, i.e. O(5%) errors, and KMN tensor FFs with O(20%) uncertainties***
   - ***assumption: broad charmonia play an entirely negligible role at high-q2***

Motivated by precision on $D_s \to \gamma$ FFs as from the lattice study **PRD '23 (2306.05904)**, confirmed by the $B_s \to \gamma$ results in **PRD '24 (2402.03262)**

$B_s \to \mu\mu\gamma$ as a golden channel to study NP

Main ingredients of our sensitivity study:

2. ***Experimental uncertainties:*** ***we will assume that all the backgrounds are under control, i.e. that their uncertainties will eventually fall safely below the signal yield ("no-background" hypothesis).***

Thus, the Bs → μμγ-signal uncertainty will be dominated by the sheer amount of data collected

(Many effects to be taken into account: efficiencies, optimal choice of $(q_{min})^2$, …)

3. ***Theoretical uncertainties:***
   - ***GNSV FFs with shrinked uncertainties, i.e. O(5%) errors, and KMN tensor FFs with O(20%) uncertainties***
   - ***<u>assumption</u>: broad charmonia play an entirely negligible role at high-q2***

Recall that we need to resolve

$$\delta C_9^{(\mu)} / C_9^{(\mu),\mathrm{SM}} \simeq 15\% \;\; !!$$

Motivated by precision on $D_s \to \gamma$ FFs as from the lattice study **PRD '23 (2306.05904)**, confirmed by the $B_s \to \gamma$ results in **PRD '24 (2402.03262)**

$B_s \to \mu\mu\gamma$ as a golden channel to study NP

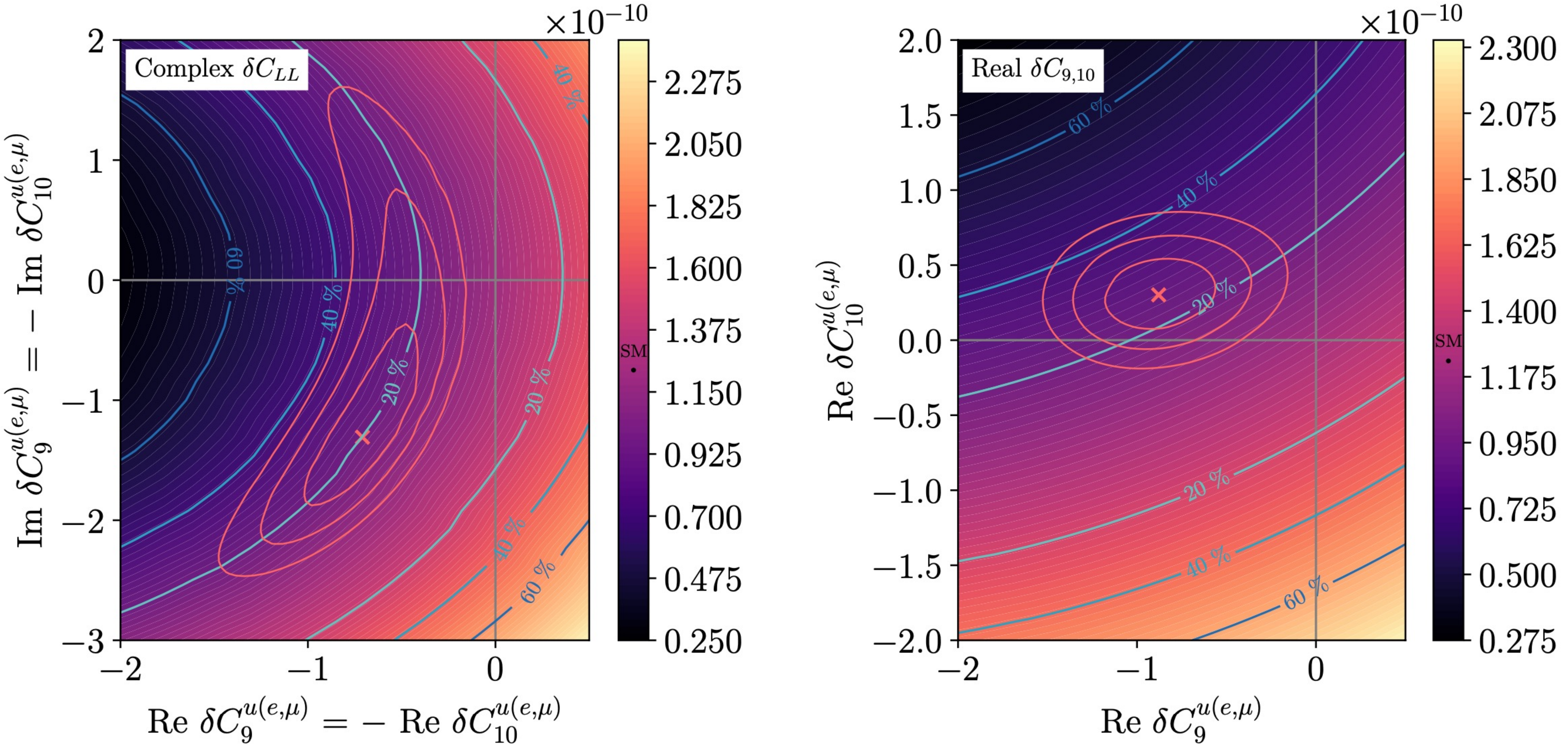

Integrated BR **for two different NP scenarios**

JHEP '23 [2308.00034]

$B_s \to \mu\mu\gamma$ as a golden channel to study NP

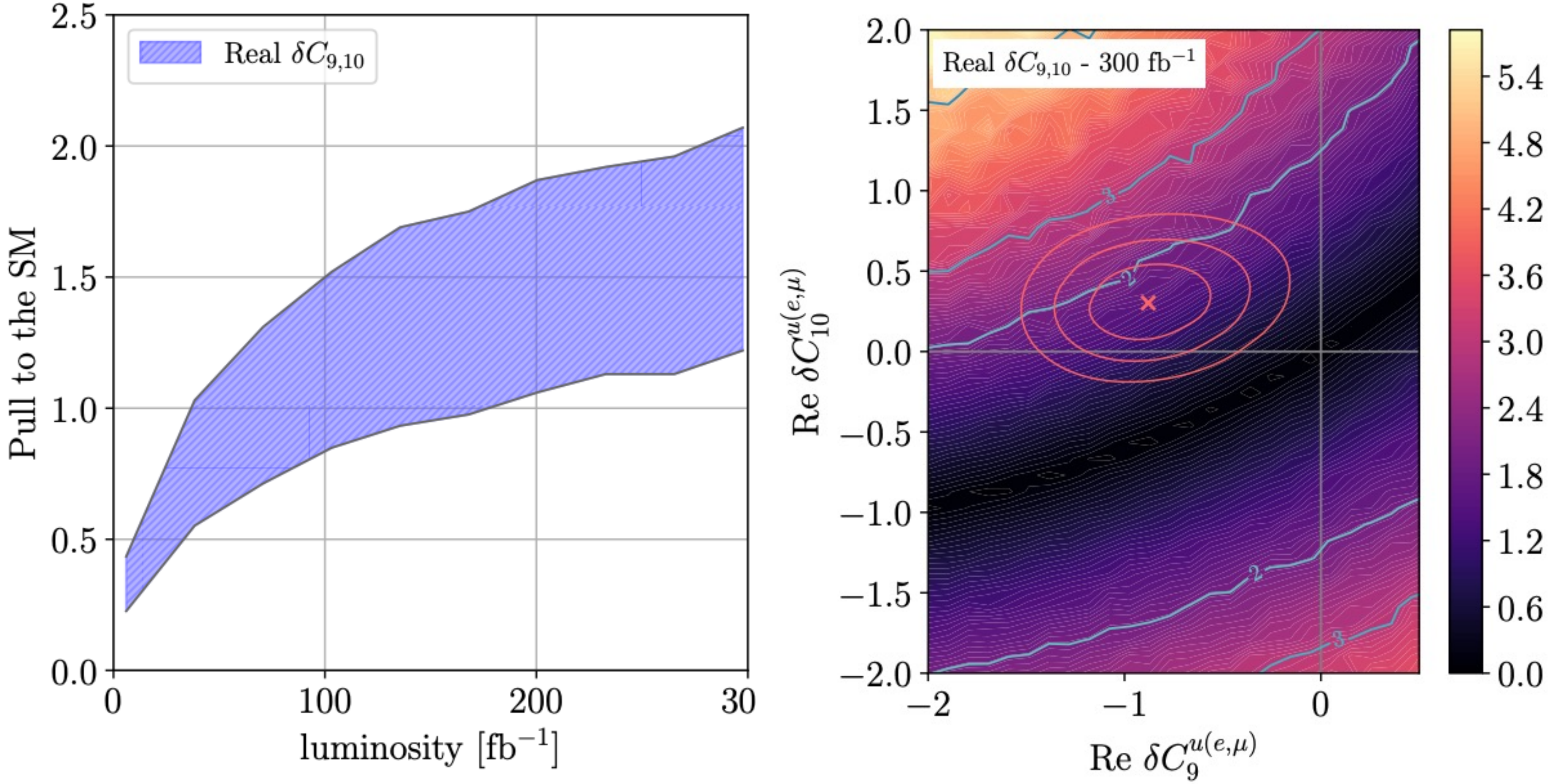

Pull to the SM of the BR **assuming NP in both C_9, C_{10}**

JHEP '23 [2308.00034]

$B_s \to \mu\mu\gamma$ as a golden channel to study NP

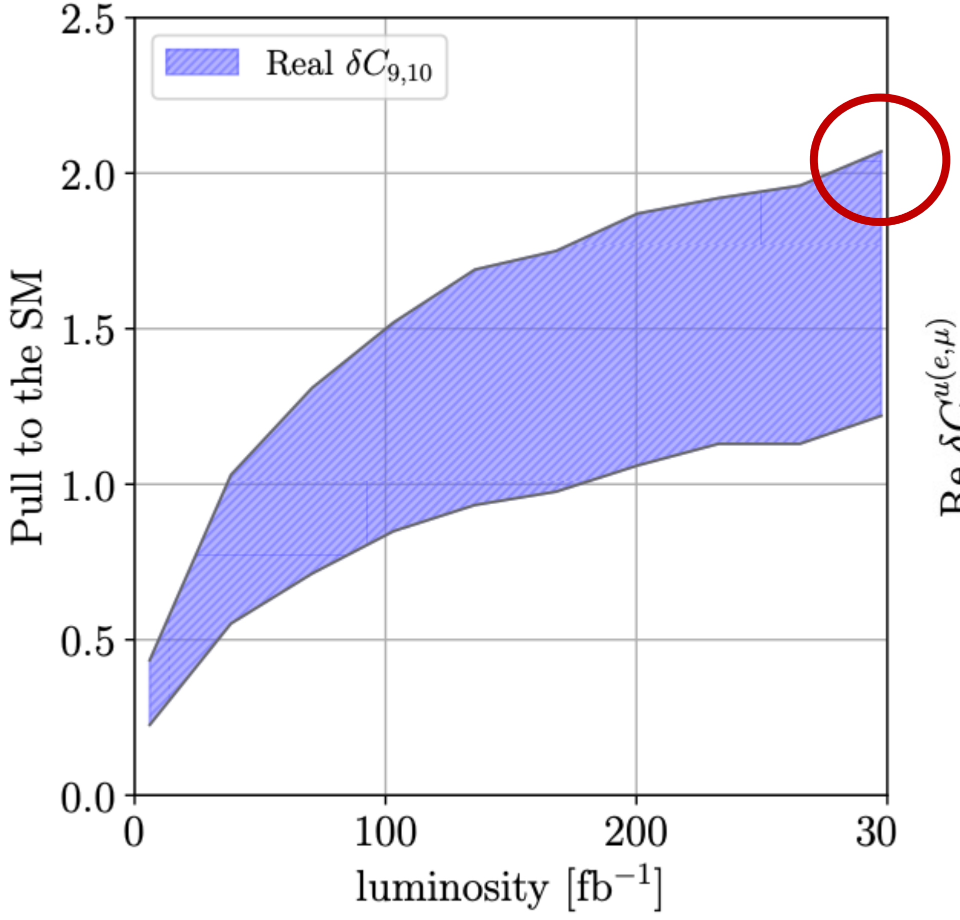

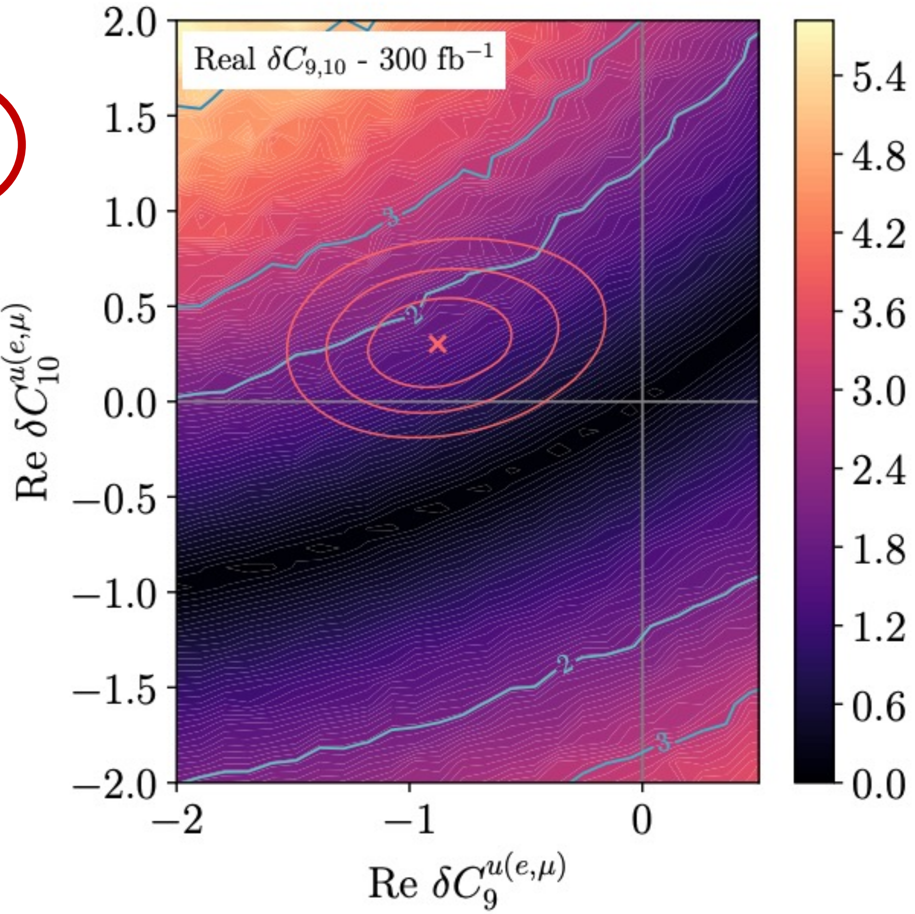

It reaches the 2σ level at the border of the 1σ region for the WC shift preferred by our global fit !

Pull to the SM of the BR **assuming NP in both C_9, C_{10}**

JHEP '23 [2308.00034]

Conclusions

Radiative-and-leptonic $B_s \rightarrow \mu\mu\gamma$ decay is an important channel to be investigated at present. Huge efforts have been and are being developed by both the theoretical and the experimental communities to have new data! In this talk:

Conclusions

Radiative-and-leptonic $B_s \to \mu\mu\gamma$ decay is an important channel to be investigated at present. Huge efforts have been and are being developed by both the theoretical and the experimental communities to have new data! In this talk:

1. **Study of $B_s \to \mu\mu\gamma$ within the SM:**
   - description of a HQET-based procedure to infer the behaviour of the FFs in the Bs-sector starting from LQCD data available for the Ds-sector @ high-q2
   - GNSV as a possible method for global analyses of all the lattice data available in the future
   - experiments: searches for $B_s \to \mu\mu\gamma$ through direct and indirect searches

Conclusions

Radiative-and-leptonic $B_s \to \mu\mu\gamma$ decay is an important channel to be investigated at present. Huge efforts have been and are being developed by both the theoretical and the experimental communities to have new data! In this talk:

1. **Study of $B_s \to \mu\mu\gamma$ within the SM:**
   - **description of a HQET-based procedure to infer the behaviour of the FFs in the Bs-sector starting from LQCD data available for the Ds-sector @ high-q2**
   - **GNSV as a possible method for global analyses of all the lattice data available in the future**
   - **experiments: searches for $B_s \to \mu\mu\gamma$ through direct and indirect searches**

2. **Study of $B_s \to \mu\mu\gamma$ beyond the SM:** complementary way to investigate hypothetical New Physics (NP) effects affecting *$b \to s$ quark transitions*
   - ***key issue*: same short-distance effects present in semileptonic neutral-current B decays, while being independent (and free) of the long-distance ones !**
   - **the pull to the SM can reach the *2σ level* at the border of the 1σ region for the WC C_9 shift preferred by our global fit of BRs and angular observables in B \to K(*) decays**
   - **assumption on the exp./th. uncertainties improvable in the future**

THANKS FOR YOUR ATTENTION !

ETMC lattice computation of FFs

The results on the FFs by ETMC have O(%) level of precision !!
(differences observed w.r.t. previous estimates, especially in $V_\perp$)

At this level of precision, the current uncertainties on charmonia effects have a non-negligible impact on the BR:

$$C_9 \;\to\; C_9 \;-\; \frac{9\pi}{\alpha^2}\,\bar{C}\,\sum_V |\eta_V| e^{i\delta_V}\,\frac{\hat{m}_V\,\mathcal{B}(V\to\mu^+\mu^-)\,\hat{\Gamma}^V_{\rm tot}}{\hat{q}^2-\hat{m}_V^2+i\hat{m}_V\hat{\Gamma}^V_{\rm tot}}$$

Frezzotti et al, PRD '24 (2402.03262)

Since $|\bar{C}|$ = 0.2, **the error on charming-penguin becomes more important than the FFs uncertainties !**

Values of the WCs taken from ***Beneke et al, JHEP '20 (2008.12494)]***

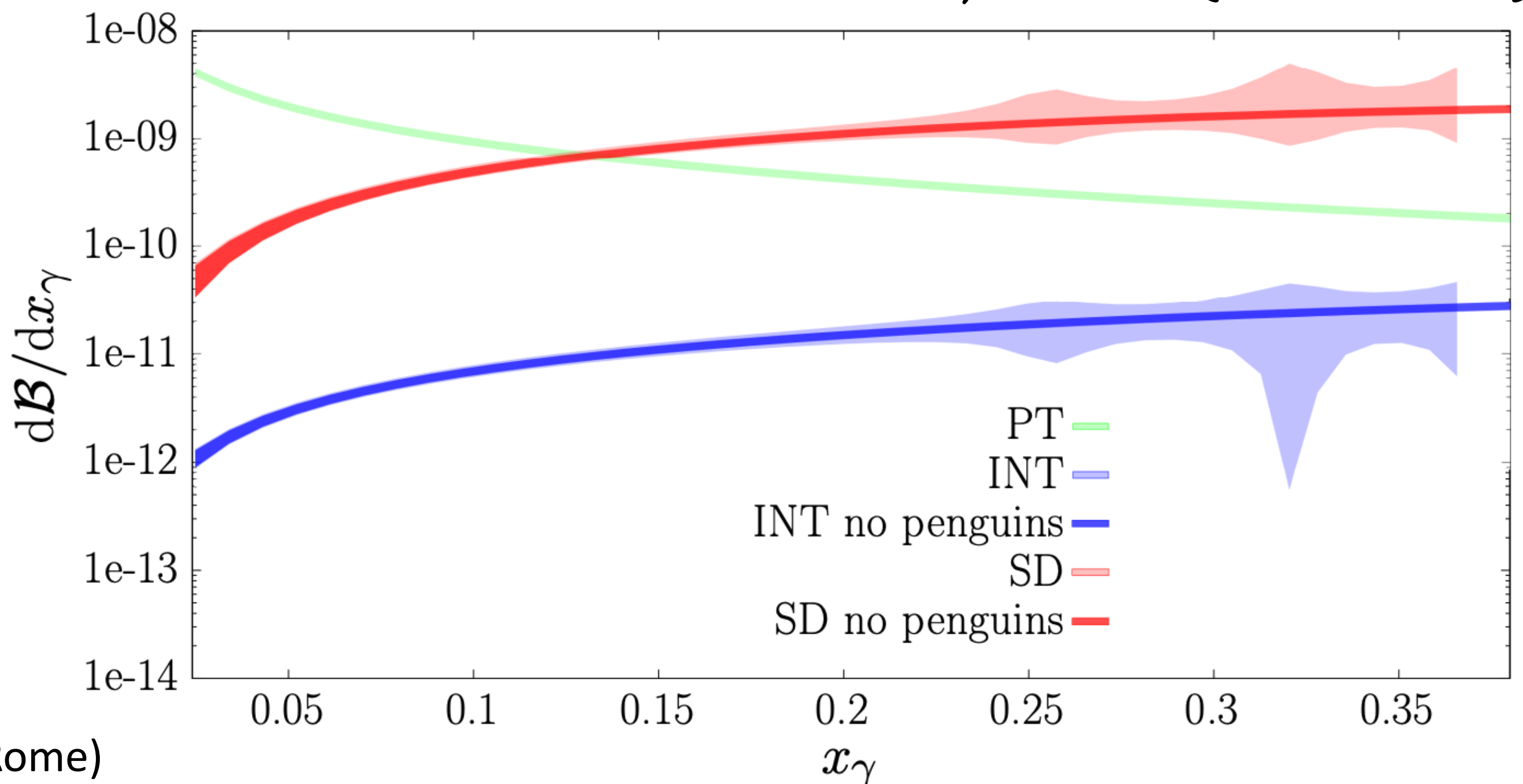

Final results for the BR prediction

Negligible impact of tensor FFs …

$\mathcal{B}(B_s^0 \to \mu^+\mu^-\gamma)[4.2\ \text{GeV}, m_{B_s^0}]$	
GNSV	$(1.63 \pm 0.80) \times 10^{-10}$
KMN [6]	$(1.83 \pm 0.69) \times 10^{-10}$
JPZ [7]	$(1.90 \pm 0.53) \times 10^{-9}$
Influence of the choice of $T_{\perp,\parallel}$ (with $V_{\perp,\parallel}$ from this work)	
$T_{\perp,\parallel}$ from KMN	$(1.22 \pm 0.70) \times 10^{-10}$
$T_{\perp,\parallel}$ from JPZ	$(0.92 \pm 0.58) \times 10^{-10}$
$T_{\perp,\parallel} = 0$	$(1.63 \pm 0.80) \times 10^{-10}$

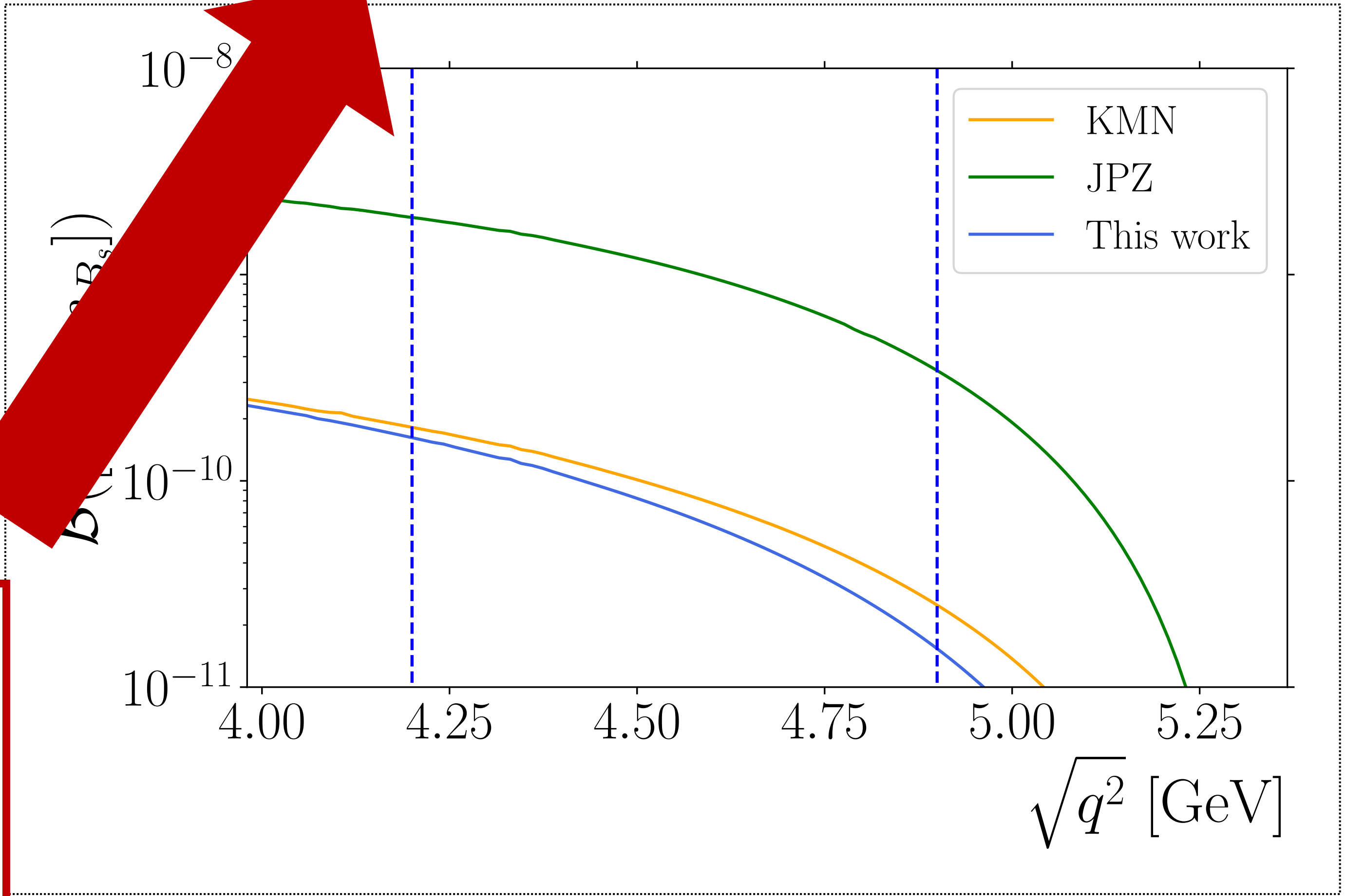

Guadagnoli, Normand, Simula, LV, JHEP '23 (2303.02174)

[3] = JPZ
[4] = KMN
[5] = GNSV

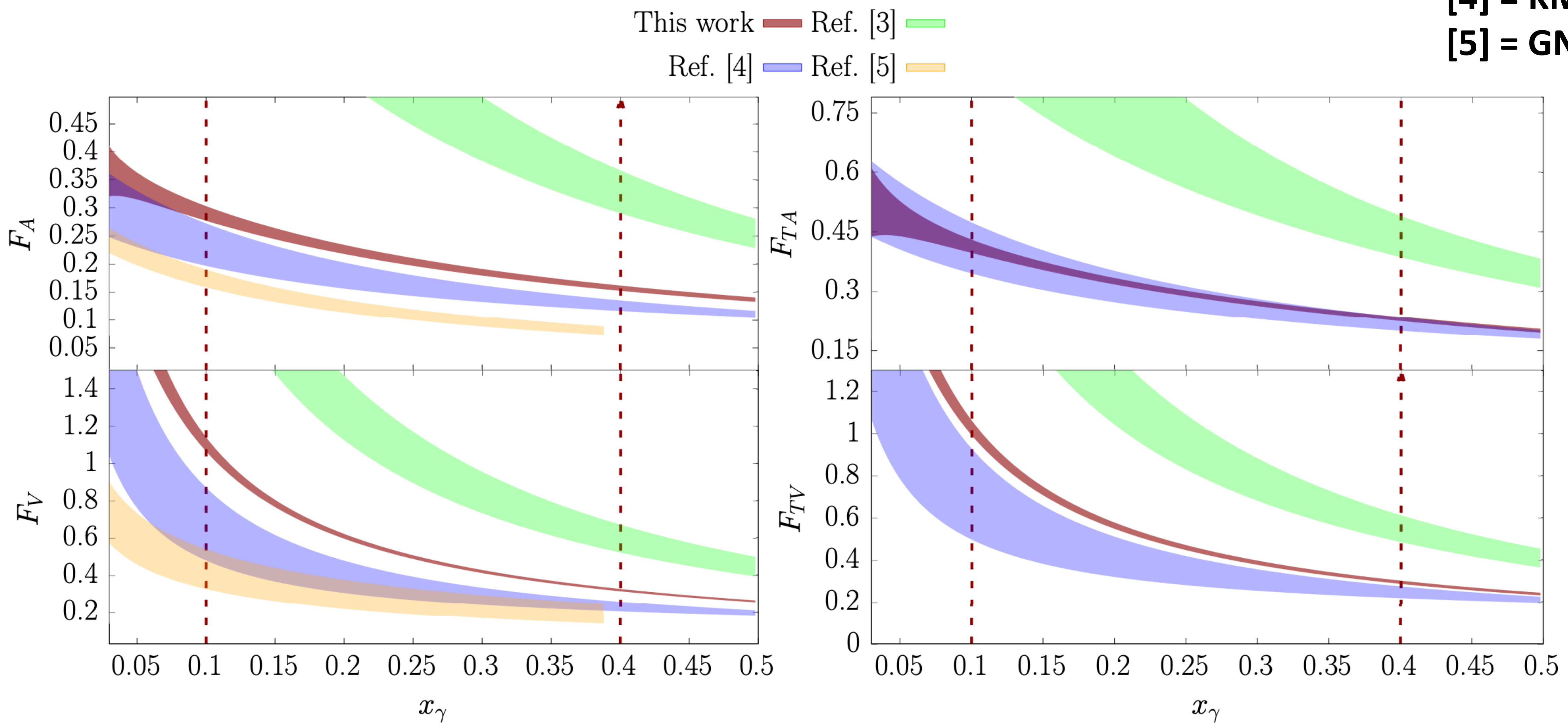

Frezzotti et al, PRD '24 (2402.03262)

ETMC lattice computation of FFs

The relevant hadronic contributions to be computed can come from (recalling the structure of the Hamiltonian):

- Semileptonic operators

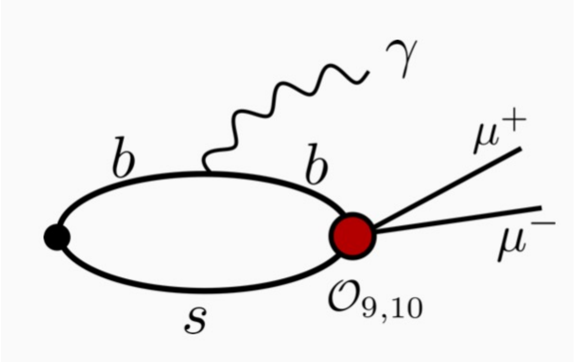

- Photon-penguin operator

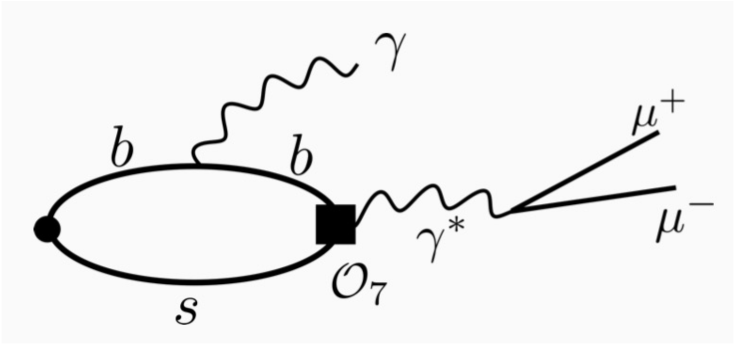

- Four-quark operators

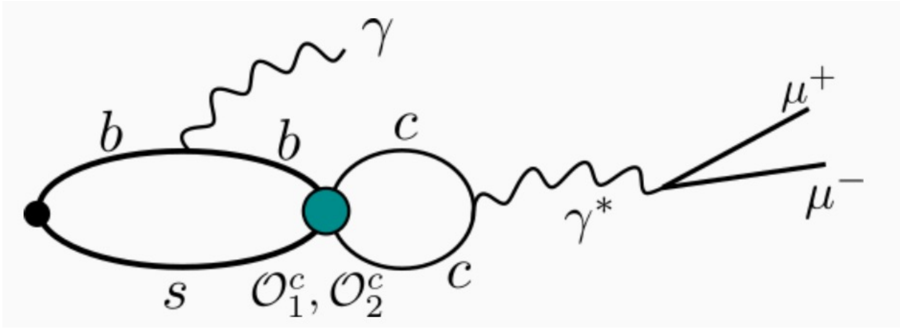

Example of diagrams taken from ***Frezzotti et al, PRD '24 (2402.03262)***

Not computed in 2402.03262 (future plans to do so)

Two extrapolations to be performed :

i) Continuum extrapolation: four values of the lattice spacing using ETMC configurations

ii) Extrapolation to the physical Bs meson mass: five different values of the heavy-strange meson mass at which simulations have been developed

ETMC lattice computation of FFs

To perform the extrapolation ii), a phenomenological fit Ansatz has been used: it combines the scaling laws valid for very hard photons [Beneke et al, EPJC '11 (1110.3228) and JHEP '20 (2008.12494)], with the quasi-pole correction due to resonance contributions (through VMD and HQET-scaling laws).

The global fit Ansatz

We extrapolate to the physical B_s through a combined fit of the form factors [$z = 1/m_{H_s}$, fit parameters are in red]:

$$\frac{F_V(x_\gamma, z)}{f_{H_s}} = \frac{|q_s|}{x_\gamma} \frac{1}{1 + C_V \frac{2z^2}{x_\gamma}} \left(K + (1+\delta_z)\frac{z}{x_\gamma} + \frac{1}{z^{-1} - \Lambda_H} + A_m z + A_{x_\gamma} \frac{z}{x_\gamma} \right)$$

$$\frac{F_A(x_\gamma, z)}{f_{H_s}} = \frac{|q_s|}{x_\gamma} \frac{1}{1 + C_A \frac{2z}{x_\gamma}} \left(K - (1+\delta_z)\frac{z}{x_\gamma} - \frac{1}{z^{-1} - \Lambda_H} + A_m z + (A_{x_\gamma} + 2KC_A) \frac{z}{x_\gamma} \right)$$

$$\frac{F_{TV}(x_\gamma, z)}{f_{H_s}} = \frac{|q_s|}{x_\gamma} \frac{1 + 2C_V z^2}{1 + C_V \frac{2z^2}{x_\gamma}} \left(K_T + (A^T_m + 1)z + A^T_{x_\gamma} \frac{z}{x_\gamma} + (1+\delta'_z) z \frac{1 - x_\gamma}{x_\gamma} \right)$$

$$\frac{F_{TA}(x_\gamma, z)}{f_{H_s}} = \frac{|q_s|}{x_\gamma} \frac{1 + 2C^T_A z}{1 + C^T_A \frac{2z}{x_\gamma}} \left(K_T + (A^T_m + 1)z + A^T_{x_\gamma} \frac{z}{x_\gamma} - (1 + \delta'_z - 2K_T C^T_A) z \frac{1 - x_\gamma}{x_\gamma} \right)$$

G.Gagliardi, presentation @ «Workshop on radiative leptonic B decays», Marseille 2024

$$\frac{F_V(x_\gamma, m_{H_s})}{f_{H_s}} = \frac{|q_s|}{x_\gamma}\left(\frac{R(E_\gamma,\mu)}{\lambda_B(\mu)} + \xi(x_\gamma, m_{H_s}) + \frac{1}{m_{H_s}x_\gamma} + \frac{|q_b|}{|q_s|}\frac{1}{m_h}\right)$$

$$\frac{F_A(x_\gamma, m_{H_s})}{f_{H_s}} = \frac{|q_s|}{x_\gamma}\left(\frac{R(E_\gamma,\mu)}{\lambda_B(\mu)} + \xi(x_\gamma, m_{H_s}) - \frac{1}{m_{H_s}x_\gamma} - \frac{|q_b|}{|q_s|}\frac{1}{m_h}\right)$$

$$\frac{F_{TV}(x_\gamma, m_{H_s},\mu)}{f_{H_s}} = \frac{|q_s|}{x_\gamma}\left(\frac{R_T(E_\gamma,\mu)}{\lambda_B(\mu)} + \xi(x_\gamma, m_{H_s}) + \frac{1-x_\gamma}{m_{H_s}x_\gamma} + \frac{|q_b|}{|q_s|}\frac{1}{m_{H_s}}\right)$$

$$\frac{F_{TA}(x_\gamma, m_{H_s},\mu)}{f_{H_s}} = \frac{|q_s|}{x_\gamma}\left(\frac{R_T(E_\gamma,\mu)}{\lambda_B(\mu)} + \xi(x_\gamma, m_{H_s}) - \frac{1-x_\gamma}{m_{H_s}x_\gamma} + \frac{|q_b|}{|q_s|}\frac{1}{m_{H_s}}\right)$$

Scaling laws valid for very hard photons [Beneke et al, EPJC '11 (1110.3228) and JHEP '20 (2008.12494)]

- Assuming vector-meson-dominance (VMD) one has ($W = \{V, A, TV, TA\}$)

$$\frac{F_W(x_\gamma, m_{H_s})}{f_{H_s}} \propto \frac{1}{\sqrt{r_W^2 + \frac{x_\gamma^2}{4}} + \frac{x_\gamma}{2} - 1} + \mathcal{O}(\frac{1}{E_\gamma}, \frac{1}{m_{H_s}})$$

$$r_V = r_{TV} = \frac{m_{H_s^*}}{m_{H_s}}\,, \qquad r_A = r_{TA} = \frac{m_{H_{s1}}}{m_{H_s}}$$

Making use of the HQET scaling laws:

$$m^2_{\bar{H}_s^*} - m^2_{\bar{H}_s} = 2\lambda_2 + \mathcal{O}\left(\frac{1}{m_h}\right)\,, \qquad \lambda_2 \simeq 0.24\ \text{GeV}^2$$

$$m_{\bar{H}_{s1}} - m_{\bar{H}_s} = \Lambda_1 + \mathcal{O}\left(\frac{1}{m_h}\right)\,, \qquad \Lambda_1 \simeq 0.5\ \text{GeV}$$

the denominator in the VMD Ansatz becomes

$$r_{V/TV} = \frac{m_{H_s^*}}{m_{H_s}} \simeq 1 + \frac{\lambda_2}{m^2_{H_s}} \implies \sqrt{r^2_{V/TV} + \frac{x_\gamma^2}{4}} + \frac{x_\gamma}{2} - 1 \simeq \frac{\lambda_2}{m^2_{H_s}} + \frac{x_\gamma}{2} + \dots$$

$$r_{A/TA} = \frac{m_{H_{s1}}}{m_{H_s}} \simeq 1 + \frac{\Lambda_1}{m_{H_s}} \implies \sqrt{r^2_{A/TA} + \frac{x_\gamma^2}{4}} + \frac{x_\gamma}{2} - 1 \simeq \frac{\Lambda_1}{m_{H_s}} + \frac{x_\gamma}{2} + \dots$$

G.Gagliardi, presentation @ «Workshop on radiative leptonic B decays», Marseille 2024

Method I: with photon reconstruction

Unfortunately, the measured BR is <u>not</u> statistically significant in any of the three q^2-regions…

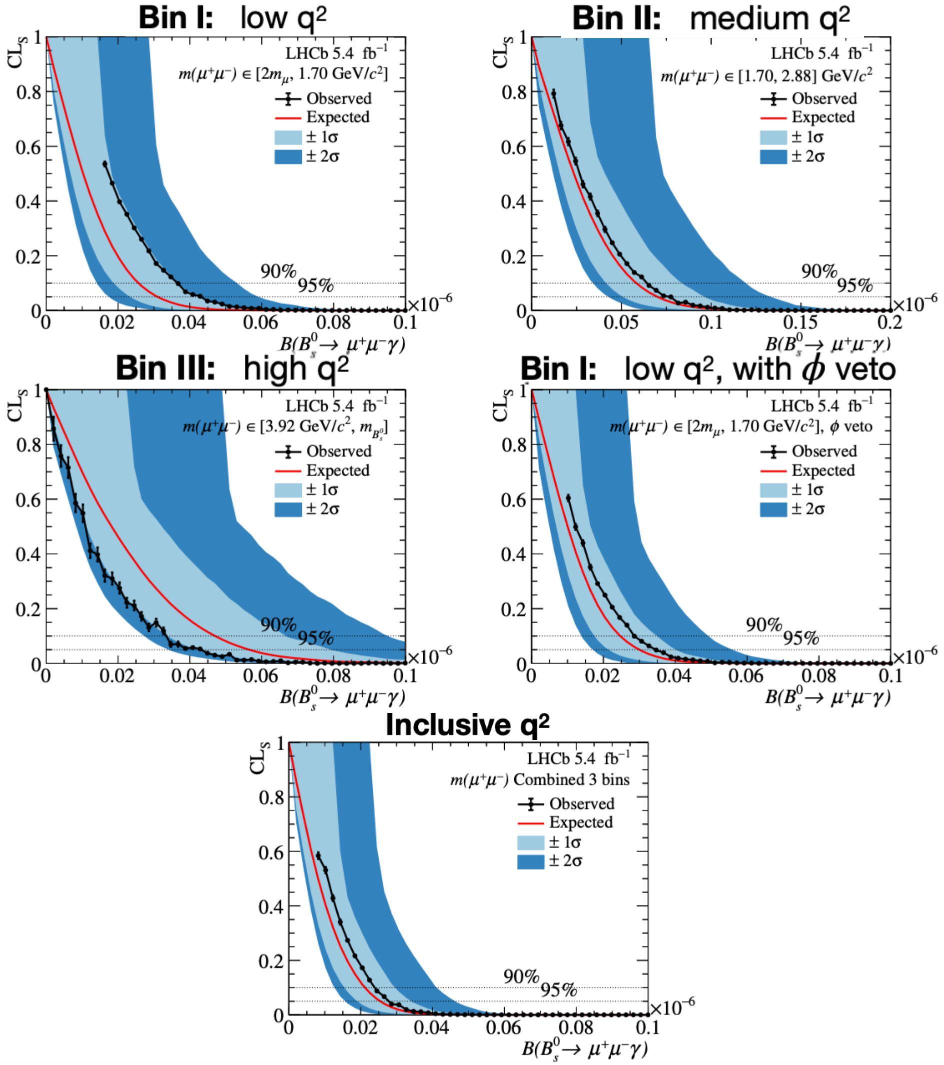

→ As no significant excess is observed, upper limits are set on $\mathscr{B}(B_s^0 \to \mu^+\mu^-\gamma)$ using the CL method.

Upper limits on the branching fraction:

$$\mathcal{B}(B_s^0 \to \mu^+\mu^-\gamma)_{\text{I}} < 3.6\,(4.2) \times 10^{-8},$$
$$\mathcal{B}(B_s^0 \to \mu^+\mu^-\gamma)_{\text{II}} < 6.5\,(7.7) \times 10^{-8},$$
$$\mathcal{B}(B_s^0 \to \mu^+\mu^-\gamma)_{\text{III}} < 3.4\,(4.2) \times 10^{-8},$$
$$\mathcal{B}(B_s^0 \to \mu^+\mu^-\gamma)_{\text{I},\,\phi\ \text{veto}} < 2.9\,(3.4) \times 10^{-8},$$
$$\mathcal{B}(B_s^0 \to \mu^+\mu^-\gamma)_{\text{comb.}} < 2.5\,(2.8) \times 10^{-8},$$

at 90% (95%) CL.

Irene Bachiller - Search for the $B_s^0 \to \mu^+\mu^-\gamma$ decay at LHCb 15

Method II: measure **Bs → $\mu\mu\gamma$** <u>without</u> photon reconstruction

<u>In short:</u> to the extent that the FSR contribution can be systematically subtracted off, as is the case for leptonic Bs searches, **one can measure the *ISR* component of the radiative-and-leptonic spectrum – and thereby the differential rate of this process – as "contamination" of the non-radiative candidate events (as the signal window is enlarged downwards)**

$$\mathcal{B}(B_s^0 \to \mu^+\mu^- + n\gamma) \quad \textbf{VS} \quad \mathcal{B}(B_s^0 \to \mu^+\mu^-\gamma)$$

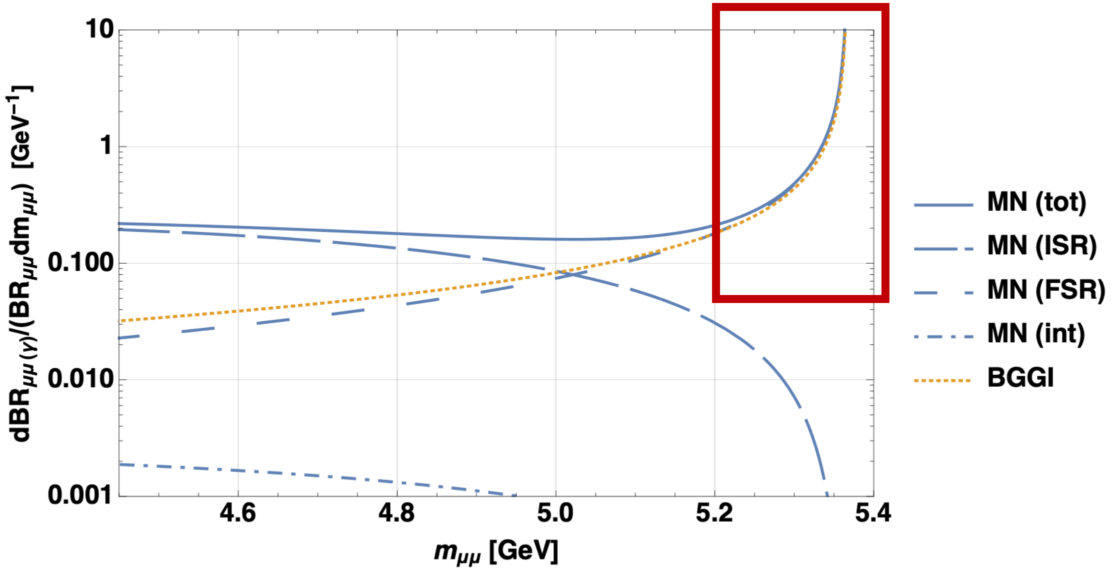

For very soft photons, the single-photon component of the former should be equal to the latter!

MN = Melikhov, Nikitin, PRD '04 [hep-ph/0410146]

BGGI = Buras, Girrbach, Guadagnoli, Isidori, EPJC '12 [1208.0934]

Bin I: low q²

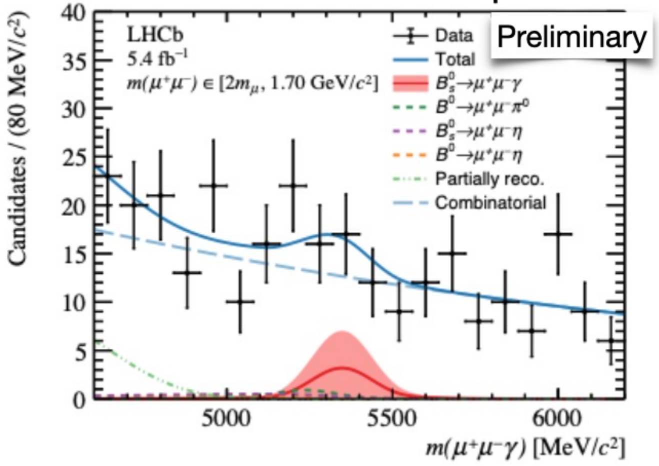

Bin II: medium q²

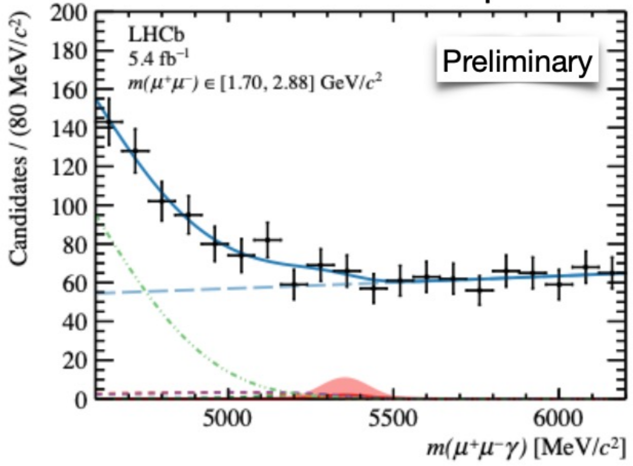

The measured $\mathcal{B}(B_s^0 \to \mu^+\mu^-\gamma)$ is not statistically significant in any of the q² regions.

Bin III: high q²

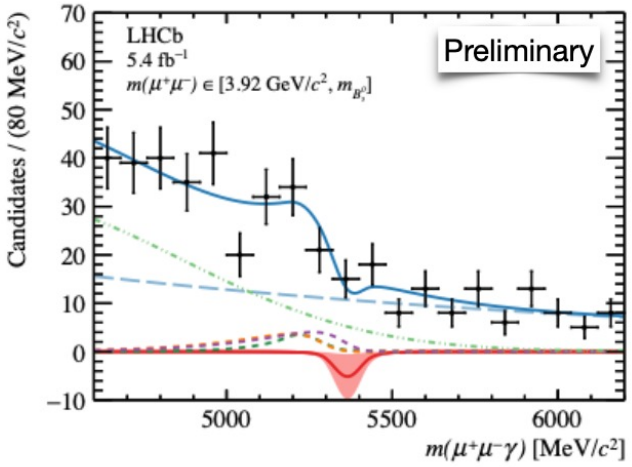

Bin I: low q², with ϕ veto

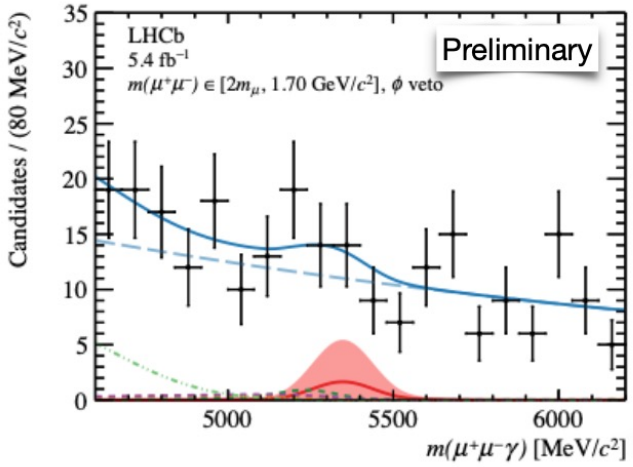

They are consistent with the background-only hypothesis at < 1σ level.

$$
\begin{aligned}
\mathcal{B}(B_s^0 \to \mu^+\mu^-\gamma)_{\mathrm{I}} &= (1.34 \pm 1.60 \pm 0.28) \times 10^{-8}, \\
\mathcal{B}(B_s^0 \to \mu^+\mu^-\gamma)_{\mathrm{II}} &= (0.76 \pm 3.55 \pm 0.30) \times 10^{-8}, \\
\mathcal{B}(B_s^0 \to \mu^+\mu^-\gamma)_{\mathrm{III}} &= (-2.55 \pm 2.25 \pm 0.41) \times 10^{-8}, \\
\mathcal{B}(B_s^0 \to \mu^+\mu^-\gamma)_{\mathrm{I},\ \phi\ \mathrm{veto}} &= (0.72 \pm 1.56 \pm 0.29) \times 10^{-8}.
\end{aligned}
$$

stat.±syst.

Dominated by statistical uncertainty.

I. Bachiller, presentation @ «Workshop on radiative leptonic B decays», Marseille 2024

Soft-photon correction for Bs \to \mu+ \mu-

$$\mathcal{B}^{\rm phys}(E_{\rm max}) \equiv \mathcal{B}(B_s \to \mu^+\mu^- + n\gamma)|_{\sum E_\gamma \leq E_{\rm max}} \quad \Longrightarrow \quad \mathcal{B}^{\rm phys}(E_{\rm max}) = \omega(E_{\rm max}) \times \mathcal{B}^{(0)}$$

In the soft-photon approximation:

$$\begin{aligned} \omega(E_{\rm max}) &= \omega_{\rm IB}(E_{\rm max}) \times \left[1 + O\left(\frac{\alpha_{\rm em}}{\pi}\right)\right] , \\ \omega_{\rm IB}(E_{\rm max}) &= \left(\frac{2E_{\rm max}}{m_{B_s}}\right)^{\frac{2\alpha_{\rm em}}{\pi} b} , \end{aligned}$$

where

$$b \equiv -\left[1 - \frac{1}{2\beta_{\mu\mu}} \ln\left(\frac{1+\beta_{\mu\mu}}{1-\beta_{\mu\mu}}\right)\right] , \qquad \beta_{\mu\mu} = \left[1 - \frac{4m_\mu^4}{(m^2_{\mu^+\mu^-} - 2m_\mu^2)^2}\right]^{1/2} \qquad E_{\rm max} = \frac{m^2_{B_s} - m^2_{\mu^+\mu^-}}{2m_{B_s}}$$

Order 10% suppression of the non-radiative rate !

Relevant data for $b \to s$ global fits

$\boldsymbol{b \to s\mu^+\mu^-}$ **BR obs.**
$\left\langle \frac{d\mathcal{B}}{dq^2} \right\rangle (B^+ \to K^{(*)}\mu\mu)$
$\left\langle \frac{d\mathcal{B}}{dq^2} \right\rangle (B_0 \to K\mu\mu)$
$\left\langle \frac{d\mathcal{B}}{dq^2} \right\rangle (B_s \to \phi\mu\mu)$
$\left\langle \frac{d\mathcal{B}}{dq^2} \right\rangle (B_0 \to K^*\mu\mu)$
$\langle \mathcal{B} \rangle (B \to X_s\mu\mu)$
$\boldsymbol{b \to s\mu^+\mu^-}$ **angular and CPV obs.**
$\langle F_L, P_1, P'_{4,5}, A_{\mathrm{FB}} \rangle (B_0 \to K^*\mu^+\mu^-)$
$\langle F_L, P_{1,2}, P'_{4,5} \rangle (B^+ \to K^{*+}\mu^+\mu^-)$
$\langle F_L, S_{3,4,7} \rangle (B_s \to \phi\mu\mu)$
$A_{3-9}(B_0 \to K^*\mu^+\mu^-)$

$\boldsymbol{R_{K/K^*}}$
$\boldsymbol{\mathcal{B}(B_{d,s} \to \mu\mu)}$
$\boldsymbol{b \to s\gamma}$ **obs.**
$\langle \mathcal{B}, A_{CP} \rangle (B \to X_s\gamma)$
$\mathcal{B}(B^0 \to K^{*0}\gamma)/\mathcal{B}(B_s^0 \to \phi\gamma)$
$\mathcal{B}(B \to K^*\gamma)$
$\mathcal{B}(B_s^0 \to \phi\gamma)$
$A_{\Delta\Gamma}, S(B_s^0 \to \phi\gamma)$
$S_{K^{*0}\gamma}$

Disappearance of R(K) and R(K*) anomalies

Analysis: results

Results

$$\text{low-}q^2 \begin{cases} R_K = 0.994\,^{+0.090}_{-0.082}\,(\text{stat})\,^{+0.027}_{-0.029}\,(\text{syst}), \\ R_{K^*} = 0.927\,^{+0.093}_{-0.087}\,(\text{stat})\,^{+0.034}_{-0.033}\,(\text{syst}) \end{cases}$$

$$\text{central-}q^2 \begin{cases} R_K = 0.949\,^{+0.042}_{-0.041}\,(\text{stat})\,^{+0.023}_{-0.023}\,(\text{syst}), \\ R_{K^*} = 1.027\,^{+0.072}_{-0.068}\,(\text{stat})\,^{+0.027}_{-0.027}\,(\text{syst}). \end{cases}$$

- Most precise and accurate LFU test in $b \to s\ell\ell$ transition
- Compatible with SM with a simple χ^2 test on 4 measurement at 0.2 σ

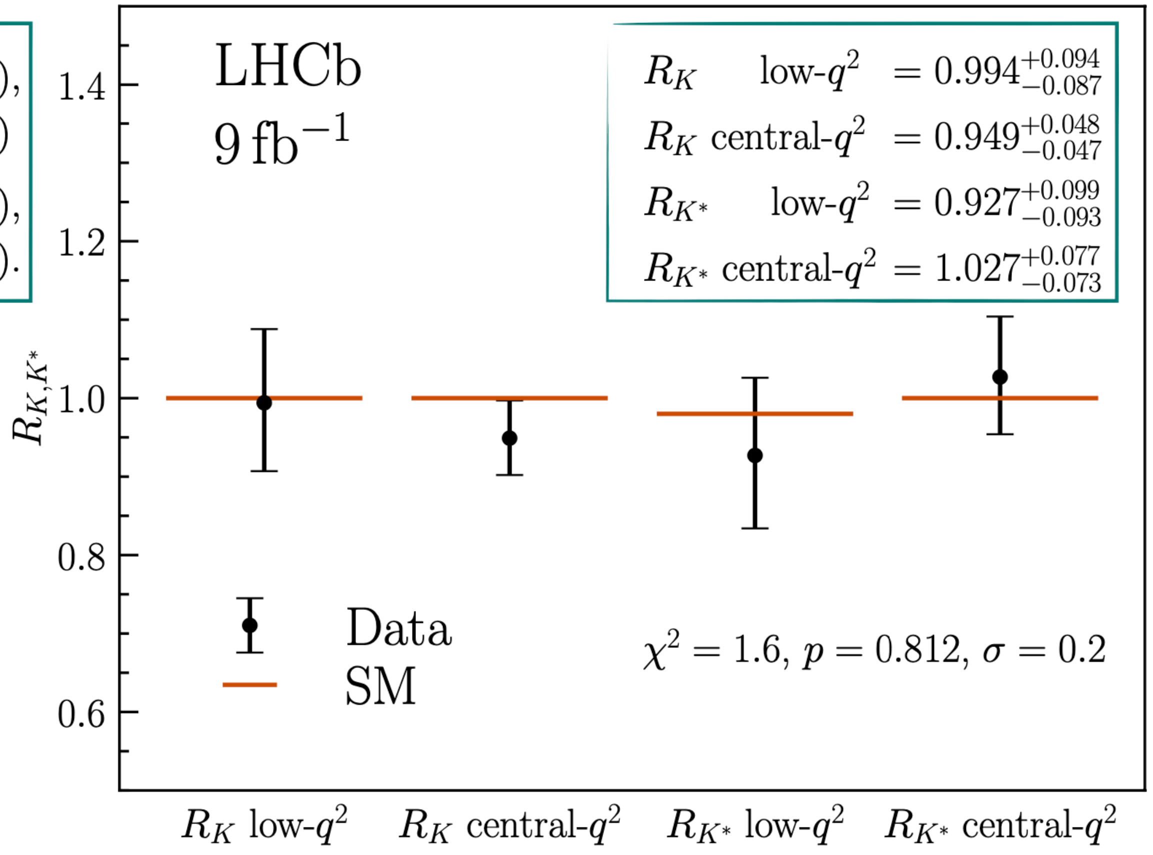

R. Quagliani's talk @ CERN, December the 20th

Other plots concerning fits to the WCs